
MODELING HETEROGENEITY AND MISSING DATA OF MULTIPLE LONGITUDINAL OUTCOMES IN ELECTRONIC HEALTH RECORDS

A PREPRINT

Rebecca Anthopolos

Division of Biostatistics, Department of Population Health
New York University Grossman School of Medicine
New York, NY
rebecca.anthopolos@nyulangone.org

Ying Wei

Department of Biostatistics
Columbia University Mailman School of Public Health
New York, NY
yw2148@cumc.columbia.edu

Qixuan Chen

Department of Biostatistics
Columbia University Mailman School of Public Health
New York, NY
qc2138@cumc.columbia.edu

March 23, 2021

ABSTRACT

In electronic health records (EHRs), latent subgroups of patients may exhibit distinctive patterning in their longitudinal health trajectories. For such data, growth mixture models (GMMs) enable classifying patients into different latent classes based on individual trajectories and hypothesized risk factors. However, the application of GMMs is hindered by the special missing data problem in EHRs, which manifests two patient-led missing data processes: the visit process and the response process for an EHR variable conditional on a patient visiting the clinic. If either process is associated with the process generating the longitudinal outcomes, then valid inferences require accounting for a nonignorable missing data mechanism. We propose a Bayesian shared parameter model that links GMMs of multiple longitudinal health outcomes, the visit process, and the response process of each outcome given a visit using a discrete latent class variable. Our focus is on multiple longitudinal health outcomes for which there can be a clinically prescribed visit schedule. We demonstrate our model in EHR measurements on early childhood weight and height z-scores. Using data simulations, we illustrate the statistical properties of our method with respect to subgroup-specific or marginal inferences. We built the R package `EHRmiss` for model fitting, selection, and checking.

Keywords Electronic health records · Gibbs sampling · Latent class modeling · Missing not at random · Multiple longitudinal health outcomes · Shared parameter model

1 Introduction

As electronic health records (EHRs) are increasingly adopted in US health systems, an estimated one billion patient visits may be documented per year [Hripcsak and Albers, 2013]. Thanks to the rapid advancement of big data management and processing, EHRs are often computable, representing an exceptional observational data resource for new discoveries in science and medicine. A natural feature of such big data may be unobserved, or “latent” heterogeneity, whereby latent subgroups of patients are characterized by distinctive patterning in their longitudinal health trajectories. Researchers from diverse biomedical fields, such as psychology [Elliott et al., 2005] and maternal and infant health [Neelon et al., 2011], have used growth mixture models (GMMs) [Muthen et al., 2002, Verbeke and Lesaffre, 1996] to analyze latent

heterogeneity in longitudinal data from diverse data sources other than EHRs. GMMs enable classifying subjects into different subgroups, often called latent classes, according to individual longitudinal trajectories and risk factors hypothesized to be associated with class membership.

Despite the utility of GMMs for EHR-based research, their application is hindered by the special missing data problem in EHRs. In the prototypical mixed model for longitudinal data analysis [Laird and Ware, 1982], missed measurements are assumed to be missing at random (MAR). However, this assumption may not be valid in EHRs due to the presence of two patient-led missing data processes. First, a patient’s *visit process*, defined as the probability of observing a clinic visit at a given time, is driven by some combination of a patient’s own prerogative and physician recommendation. The second missing data process is the response process given a clinic visit, defined by the conditional probability of observing a response on an EHR variable given a clinic visit. In EHRs, the likelihood that a variable gets investigated – and in turn, recorded – may depend on a patient’s stated medical reasons for the visit, in addition to clinical judgment. When either missing data process is associated with the underlying process generating the longitudinal health outcomes, then valid inferences for any models require accounting for a missing not at random (MNAR) mechanism. To our knowledge, no methods have been developed to fully accommodate a two-fold MNAR mechanism in EHRs.

In the missing data literature, a visit process that is associated with the underlying process generating the longitudinal outcomes has been characterized as a special case of MNAR known as “informative” [Wu and Carroll, 1988, Follmann and Wu, 1995]. A common approach to handling an informative visit process is a shared parameter framework [Wu and Carroll, 1988, Follmann and Wu, 1995]. It assumes that the distributions of the longitudinal outcomes and visit process *share* a continuous or discrete latent variable, which drives the correlation between missed visits and longitudinal outcomes. Once conditioning on the latent variable, the longitudinal outcomes and visit process are assumed to be independent [Liang et al., 2009, Sun et al., 2007, McCulloch et al., 2016, Lin et al., 2004]. However, existing shared parameter models are insufficient to describe the complexity of EHRs where the response process of individual health outcomes given a clinic visit may also exhibit an MNAR mechanism.

To apply growth mixture modeling to longitudinal health outcomes collected in EHRs, we propose a Bayesian shared parameter model, which integrates GMMs of the longitudinal health outcomes, the visit process, and the response process of individual health outcomes given a clinic visit, using a discrete latent variable to indicate the latent class to which each patient belongs. Our focused applications are preventive care (e.g., screenings for cholesterol) and chronic disease management (e.g., HbA1c % among patients with type 2 diabetes) in which certain health outcomes are routinely collected with a clinically prescribed visit schedule. We demonstrate our proposed model with early childhood weight and height measurements, which should be collected according to the well-child check schedule [American Academy of Pediatrics, 2018]. Using the prescribed visit schedule, we construct time windows of observation to measure each patient’s visit process, and in turn, response process for each health outcome. We developed an efficient Markov chain Monte Carlo (MCMC) algorithm based on easily sampled closed-form full conditional distributions. To conduct model fitting, selection, and checking, we built the user-friendly R package `EHRMiss` available at <https://github.com/anthopolos/EHRMiss>.

2 Statistical Method

We formulate our proposed Bayesian shared parameter model of longitudinal health outcomes collected in EHRs. First, in Section 2.1, we present the complete-data model. In Section 2.2, we extend the complete-data model to account for a nonignorable visit process and response process given a clinic visit. Lastly, in Section 2.3, we explicate our Bayesian computation.

2.1 Complete-data model

Suppose there are K latent classes of patients with distinctive patterning in their trajectories of R health outcomes collected over J prescribed clinical time windows. The complete-data model is a Bayesian multivariate GMM with submodels for latent class membership and the longitudinal health outcomes. We begin with latent class membership. Let c_i be a discrete latent variable taking values $k = 1, \dots, K$ to indicate the latent class membership of patient i for $i = 1, \dots, n$. We assume that

$$c_i \sim \text{Multinomial}(1; \pi_{i1}, \dots, \pi_{iK}), \quad (1)$$

where π_{ik} are patient-specific latent class membership probabilities. To connect π_{ik} with covariates of interest, we introduce K latent random variables ξ_{ik}^* ($k = 1, \dots, K$) such that $\pi_{ik} = Pr(\xi_{ik}^* > \xi_{il}^* \text{ for all } l \neq k)$. Upon defining latent class K as the reference level by setting $\xi_{ik} = \xi_{ik}^* - \xi_{iK}^*$ for $k = 1, \dots, K - 1$, we specify the following model:

$$\xi_{ik} = \mathbf{w}_i \delta_k^T + \epsilon_{ik} \quad \text{and} \quad c_i = \begin{cases} K & \text{if } \max(\xi_{i1}, \dots, \xi_{iK-1}) < 0 \\ k & \text{if } \max(\xi_{i1}, \dots, \xi_{iK-1}) = \xi_{ik} \geq 0. \end{cases} \quad (2)$$

In (2), \mathbf{w}_i is a $1 \times s$ row vector containing a one for an intercept and $s - 1$ covariates, such as patient-level risk factors, with corresponding regression coefficients in δ_k . The ϵ_{ik} are normal random errors with mean zero and identity variance-covariance matrix [StataCorp, 2019]. For $K = 2$, this set-up corresponds to the standard Bayesian probit model for a binary outcome [Albert and Chib, 1993].

The multivariate model of longitudinal health outcomes is then specified conditional on c_i . Let y_{1ij}, \dots, y_{Rij} be longitudinal measurements on R health outcomes for patient $i, i = 1, \dots, n$, in time window $j, j = 1, \dots, J$. Then,

$$\begin{bmatrix} y_{1ij} \\ \vdots \\ y_{Rij} \end{bmatrix} \Big|_{c_i = k} \sim MVN_R \left(\begin{bmatrix} \beta_{1k} \mathbf{x}_{ij}^T + \mathbf{b}_{1i} \mathbf{z}_{ij}^T \\ \vdots \\ \beta_{Rk} \mathbf{x}_{ij}^T + \mathbf{b}_{Ri} \mathbf{z}_{ij}^T \end{bmatrix}, \boldsymbol{\Sigma}_k \right) \quad (3)$$

$$\begin{bmatrix} \mathbf{b}_{1i} \\ \vdots \\ \mathbf{b}_{Ri} \end{bmatrix} \Big|_{c_i = k} \sim MVN_{Rq} \left(\begin{bmatrix} \mathbf{0} \\ \vdots \\ \mathbf{0} \end{bmatrix}, \boldsymbol{\Psi}_k \right). \quad (4)$$

In (3), conditional on c_i , y_{rij} ($r = 1, \dots, R$) are modeled as a smooth function of time in window j , with \mathbf{x}_{ij}^T being a p -length column vector containing a one and $(p - 1)$ polynomial terms for time. The corresponding regression coefficients in β_{rk} capture the average trajectory for health outcome r in latent class k . Covariates other than time may be included in \mathbf{x}_{ij} . The $\boldsymbol{\Sigma}_k$ is an $R \times R$ latent class-specific residual variance-covariance among y_{rij} ($r = 1, \dots, R$).

For each longitudinal health outcome r , \mathbf{b}_{ri} is a $1 \times q$ row vector of patient-specific random effects associated with \mathbf{z}_{ij}^T , the columns of which are a subset of \mathbf{x}_{ij}^T . As shown in (4), \mathbf{b}_{ri} are modeled given c_i , thus reflecting patient-specific variability around the average health trajectory in latent class k . The latent class-specific variance-covariance $\boldsymbol{\Psi}_k$ in (4) is an $Rq \times Rq$ block diagonal matrix with entries $\boldsymbol{\Psi}_{kr}$ ($q \times q$), the elements of which compose a variance-covariance for \mathbf{b}_{ri} ($i = 1, \dots, n$). For simplicity, we have used the same \mathbf{x}_{ij} and \mathbf{z}_{ij} for each longitudinal health outcome y_{rij} ($r = 1, \dots, R$), but this is not required.

2.2 Nonignorable missing data processes in EHRs

We extend the complete-data model in (1) - (4) to account for nonignorable missing data mechanisms for the visit process and the response process given a clinic visit in EHRs.

To specify the full data, for health outcome r , consider the elements y_{ri1}, \dots, y_{riJ} for patient i over J time windows. Let d_{ij} ($j = 1, \dots, J$) be an indicator for the visit process such that $d_{ij} = 1$ if patient i has a clinic visit during time window j , and 0 otherwise. The response process for the r^{th} health outcome given a clinic visit is defined for the subset of time windows when patient i visits the clinic. Let $A = \{j : d_{ij} = 1 \text{ for } j = 1, \dots, J\}$, and let the total number of clinic visits for patient i be $n_i = \sum_{j=1}^J d_{ij}$. Then, for $l = 1, \dots, n_i$, define $m_{riA(l)} = 1$ if a response is observed for health outcome r at window $A(l)$, and 0 otherwise. The full data are given by y_{rij} , d_{ij} , and $m_{riA(l)}$.

To ease computational burden in MCMC estimation, we use a probit link function in modeling the probability of a clinic visit. For patient i in time window j ,

$$[d_{ij} \mid c_i = k] \sim \text{Bernoulli} \left(\Phi \{ \mathbf{x}_{ij} \phi_k^T + \mathbf{z}_{ij} \tau_i^T \} \right) \quad (5)$$

$$[\tau_i \mid c_i = k] \sim MVN_q \left(\mathbf{0}, \boldsymbol{\Omega}_k \right), \quad (6)$$

where $\Phi\{\cdot\}$ is the cumulative distribution function of the standard normal distribution. Analogous to (3) and (4), in (5) and (6), the regression coefficients in the $p \times 1$ column vector ϕ_k^T reflect the average visit process trajectory in latent class k , with q patient-specific random effects in τ_i that capture individual-level variations within each latent class. The $\boldsymbol{\Omega}_k$ is a latent class-specific variance-covariance.

Correspondingly, the probability of response for health outcome r in $A(l)$ is specified as

$$[m_{riA(l)} \mid c_i = k] \sim \text{Bernoulli} \left(\Phi \{ \mathbf{x}_{iA(l)} \lambda_{rk}^T + \mathbf{z}_{iA(l)} \kappa_{ri}^T \} \right) \quad (7)$$

$$[\kappa_{ri} \mid c_i = k] \sim MVN_q \left(\mathbf{0}, \boldsymbol{\Theta}_{rk} \right), \quad (8)$$

where λ_{rk}^T is a $p \times 1$ column vector that represents the latent class-specific average response process for health outcome r , and the q patient-specific random effects in κ_{ri} are modeled with a latent class-specific variance-covariance $\boldsymbol{\Theta}_{rk}$. For

simplicity, in (5) and (7), we have assumed that $\mathbf{x}_{iA(l)}$ and $\mathbf{z}_{iA(l)}$ are the same as in the longitudinal health outcome model (3).

Conditional on c_i , the longitudinal health outcomes, visit process, and response process given a clinic visit are assumed to be independent. The MNAR mechanism is evident because the visit and response processes depend on missing longitudinal health outcomes indirectly through latent class membership. The proposed shared parameter model can be easily altered to an MAR mechanism for one or both of the visit process and response process given a clinic visit. For example, the visit process is MAR if $f(d_{ij}, \tau_i | c_i, rest) = f(d_{ij}, \tau_i | rest)$. Then, assuming separable parameter spaces, the visit process can be ignored in statistical analysis.

2.3 Bayesian computation

To complete the Bayesian model specification, we assign prior distributions to all of the parameters. For each parameter, we use the same prior distribution across mixture components. In the latent class membership model, we assign the probit regression coefficients δ_k in (2) the prior distribution $MVN_s(\mathbf{0}, \mathbf{I})$ such that on the probability scale, the mode of the prior probability of latent class membership is approximately $\frac{1}{K}$ [Garrett and Zeger, 2000, Elliott et al., 2005]. In the models for the longitudinal health outcomes, visit process, and response process given a clinic visit, we assign diffuse multivariate normal prior distributions for the latent class-specific regression coefficients β_{rk} in (3), ϕ_k in (5), and λ_{rk} in (7), and inverse-Wishart prior distributions for the hierarchical variance-covariances Ψ_{kr} in (4), Ω_k in (6), and Θ_{rk} in (8), respectively. In the longitudinal health outcome model (3), we also assign the observation-level variance-covariance Σ_k an inverse-Wishart prior distribution.

Let $\mathbf{y}_{iA(l)} = (y_{1iA(l)}, \dots, y_{RiA(l)})^T$, $\beta_k = (\beta_{1k}^T, \dots, \beta_{Rk}^T)^T$, and $\mathbf{b}_i = (\mathbf{b}_{1i}^T, \dots, \mathbf{b}_{Ri}^T)^T$. Assuming prior independence, we specify the joint posterior distribution as

$$\begin{aligned} & p(\mathbf{c}; \beta, \mathbf{b}, \Sigma, \Psi; \phi, \tau, \Omega; \lambda, \kappa, \Theta | \mathbf{y}, \mathbf{d}, \mathbf{m}; \mathbf{x}, \mathbf{z}, \mathbf{w}) \\ &= \prod_{k=1}^K \left\{ \prod_{i=1}^n \pi_{ik} \left[\prod_{j=1}^J f(d_{ij} | \tau_i, \phi_k) f(\tau_i | \Omega_k) \right] \right. \\ & \times \left. \prod_{l=1}^{n_i} \left(f(\mathbf{y}_{iA(l)} | \mathbf{b}_i, \beta_k, \Sigma_k) f(\mathbf{b}_i | \Psi_k) \prod_{r=1}^R f(m_{riA(l)} | \kappa_{ri}, \lambda_{rk}) f(\kappa_{ri} | \Theta_{rk}) \right) \right]^{1_{c_i=k}} \\ & \times p(\beta_k) p(\Sigma_k) p(\Psi_k) p(\phi_k) p(\Omega_k) \prod_{r=1}^R p(\lambda_{rk}) p(\Theta_{rk}) \left. \right\} \prod_{k=1}^{K-1} p(\delta_k), \end{aligned}$$

where $p(\cdot)$ indicates a prior distribution, and to simplify notation, the design matrices for d_{ij} , $\mathbf{y}_{iA(l)}$, and $m_{riA(l)}$ are suppressed.

We propose an MCMC algorithm that uses easily sampled closed-form full conditionals. Upon initialization, the algorithm iterates among the following steps:

1. For $k = 1, \dots, K - 1$, update δ_k and ξ_{ik} in (2). Compute π_{ik} for $k = 1, \dots, K$ in (1).
2. For $k = 1, \dots, K$, update β_{rk} , \mathbf{b}_{ri} , Σ_k , and Ψ_k in (3) and (4).
3. For $k = 1, \dots, K$, update ϕ_k , τ_i , and Ω_k in (5) and (6).
4. For $k = 1, \dots, K$, update λ_{rk} , κ_{ri} , and Θ_{rk} in (7) and (8).
5. Sample latent class indicators c_i for $i = 1, \dots, n$ from $Multinomial(1; p_{i1}, \dots, p_{iK})$, where p_{i1}, \dots, p_{iK} are the posterior probabilities of latent class assignment given by

$$\begin{aligned} p_{ik} &= Pr(c_i = k | \pi_{ik}; \mathbf{y}_i^*, \mathbf{b}_i; \mathbf{d}_i, \tau_i; \mathbf{m}_{1i}, \dots, \mathbf{m}_{Ri}, \kappa_{1i}, \dots, \kappa_{Ri}; rest) \\ &\propto \pi_{ik} f(\mathbf{y}_i^* | \mathbf{b}_i, \beta_k, \Sigma_k^*) f(\mathbf{b}_i | \Psi_k) f(\mathbf{d}_i | \tau_i, \phi_k) f(\tau_i | \Omega_k) \\ &\times \prod_{r=1}^R f(\mathbf{m}_{ri} | \kappa_{ri}, \lambda_{rk}) f(\kappa_{ri} | \Theta_{rk}), \end{aligned}$$

where $\mathbf{y}_i^* = (\mathbf{y}_{iA(1)}^T, \dots, \mathbf{y}_{iA(n_i)}^T)$, $\mathbf{d}_i = (d_{i1}, \dots, d_{iJ})^T$, and $\mathbf{m}_{ri} = (m_{riA(1)}, \dots, m_{riA(n_i)})^T$. Σ_k^* is an $n_i R \times n_i R$ block diagonal matrix with elements Σ_k ($R \times R$) for each $\mathbf{y}_{iA(l)}$ ($l = 1, \dots, n_i$).

The full MCMC algorithm is detailed in Section A of the supplementary material (SM).

3 Analysis of Early Childhood Weight and Height Measurements

We apply our proposed model to an illustrative dataset of EHR measurements on weight and height in a sample of US children followed from birth to age 4 years. These EHR measurements were linked to participants in the 1988 National Maternal and Infant Health Survey (NMIHS) and its 1991 Longitudinal Follow-Up, in which low birth weight infants ($<2,500$ g) were oversampled [Sanderson et al., 1988]. In this dataset, clinic visit times are available in terms of a child’s age in months. Clinical recommendation suggests that in early childhood, weight and height measurements should be collected at clinic visits classified as well-child checks [American Academy of Pediatrics, 2018]. The well-child check schedule prescribes clinic visits at age in months 1, 2, 4, 6, 9, 12, 15, 18, 24, 30, 36, and 48. To illustrate our proposed model, we used weight and height measurements from clinic visits classified as check-ups for a random sample of 500 children. We converted weight and height measurements to z-scores using a reference distribution from the Centers for Disease Control and Prevention [Centers for Disease Control and Prevention, 2019]. Of the 500 children, we excluded one child whose available measurements were flagged as biologically implausible values. SM Figure B.1 presents the patterns of observed visits and responses for weight and height given a clinic visit. Of 5,988 well-child windows (499 children \times 12 well-child windows), 67% correspond to missed visits. Among 1,983 observed visits, only 17 weight measurements are missing ($< 1\%$), whereas 207 height measurements (10%) are missing.

We analyze early childhood weight and height z-scores using three estimation methods that can be executed via our R package `EHRmiss`. First, the **MNAR** method demonstrates our proposed model: We assume both the visit process and response process for height are MNAR, while since weight z-scores are rarely missing, the response process for weight is MAR. Second, in the **MAR** method, we assume each of the missing data mechanisms is ignorable. For the **Naïve** method, we fit the complete-data model using only well-child windows in which both weight and height z-scores are observed, herein “complete pairs”. Whereas the **MNAR** and **MAR** methods include all 499 children (1,983 observed visits), the **Naïve** method uses only 471 children who have at least one complete pair, corresponding to 1,759 observed visits.

We include a child’s race, sex, and birth weight in w_i from the latent class membership submodel in (2). For weight and height z-scores, the visit process, and the response process for height z-scores given a clinic visit, we model longitudinal trajectories as a cubic polynomial function of a child’s age in months, and the patient-specific random effects are specified by a random intercept.

We ran the Gibbs sampler for 20,000 iterations discarding the first 10,000 as burn-in. Using three chains from dispersed initial values, the Gelman-Rubin diagnostic [Gelman et al., 2014] indicated model convergence with values near 1 for all parameters. In Bayesian mixture modeling, label switching is a well-known problem for posterior inference [Fruhwirth-Schnatter, 2006]. We used Stephen’s relabeling method [Stephens, 2000] to assess the label switching problem via the R package `label.switching` [Papastamoulis, 2016]. This method identifies the labeling permutation that minimizes the Kullback-Leibler divergence between the posterior probabilities of latent class assignment averaged over MCMC iterations and the corresponding probabilities at each MCMC iteration. For each GMM in our data application, the original (identity) labeling was returned, which suggests that the label switching problem was not detected.

We proceed in Section 3.1 by demonstrating the **MNAR** method in analyzing longitudinal trajectories of weight and height z-scores, the visit process, and the response process for height z-scores given a clinic visit, including selecting among models with varying numbers of latent classes and conducting model checking using the posterior predictive distribution. In Section 3.2, we use a 2-latent class model in order to simply explicate the patterns of differential child classification among the **Naïve**, **MAR**, and **MNAR** methods.

3.1 Longitudinal trajectories of weight and height z-scores using the MNAR method

A challenge in data applications with GMMs is to select among models that assume a varying number of latent classes K . We compared different K -class models based on the **MNAR** method according to model information criteria, including the Bayesian Information Criterion (BIC) [Schwarz, 1978] and a modified version of the Deviance Information Criterion (DIC) [Spiegelhalter et al., 2002] known as the DIC3 recommended for latent variable models [Celeux et al., 2006]; the log-pseudo marginal likelihood (LPML) [Geisser and Eddy, 1979, Gelfand and Dey, 1994, Ibrahim et al., 2001]; a graphical technique known as latent class identifiability displays (LCIDs) [Garrett and Zeger, 2000]; and, clinical interpretation. We selected the 3-class model. Details are provided in Section B of the SM.

Based on the 3-class model, Figure 1 shows the latent class-specific average trajectories of weight and height z-scores, the visit process, and the response process for height z-scores given a clinic visit. The longitudinal trajectories of weight and height z-scores, the visit process, and the response process for height z-scores exhibited latent heterogeneity. Using the weight trajectories to label the latent classes of children, we identified Normal, increasing (purple); Normal,

decreasing (orange); and Low (blue) subgroups. The visit process of the Normal, increasing subgroup decreases over follow-up, whereas for the Normal, decreasing subgroup, the probability of a clinic visit rises at the outset before decreasing. The probability of response for height z-scores is indistinguishable for these two subgroups. In the Low subgroup, the probability of clinic visit rises slowly over follow-up, while the response process for height z-scores climbs sharply until about 12 months. Based on the maximum of a child’s mean posterior probabilities of belonging to each latent class, we assigned approximately one-third of children to each subgroup, with subgroup mean (median) probability ranging from 0.81 to 0.84 (0.84 to 0.93) (SM Table B.2).

For model checking in the presence of missing data, we used the completed datasets that include observed and imputed weight and height z-scores in each well-child window, and replicates of the completed datasets drawn from the posterior predictive distribution [Gelman et al., 2005]. We conducted Bayesian posterior predictive checking using the multivariate mean square error [Daniels and Hogan, 2008] as our discrepancy measure,

$$T = \sum_{k=1}^K \sum_{i=1}^n \sum_{l=1}^{n_i} (\mathbf{y}_{iA(l)} - \mu_{iA(l)}) \Sigma_k^{-1} (\mathbf{y}_{iA(l)} - \mu_{iA(l)})^T \times \mathbf{1}_{c_i=k}, \quad (9)$$

where $\mu_{iA(l)} = \mathbf{x}_{iA(l)} \beta_k^T + \mathbf{z}_{iA(l)} \mathbf{b}_i^T$. SM Figure B.5 presents a scatter plot of the discrepancy measure T in (9) across MCMC samples, with the horizontal and vertical axes being T based on the completed and replicated datasets, respectively. Comparing completed and replicated T , the Bayesian predictive p-value of 0.44 suggests adequate overall model fit. In addition, we compared histograms of randomly selected completed and replicated datasets of weight and height z-scores [Gelman et al., 2005]. In SM Figures B.6 and B.7, the distribution of z-scores by subgroup and well-child window appears largely consistent between the completed and replicated datasets.

3.2 Child classification using the different estimation methods in 2-class models

Based on the simplifying assumption of two latent classes, we examine the patterns of differential child classification among the **Naïve**, **MAR**, and **MNAR** methods. Herein, after briefly describing analysis results under each method, we focus our presentation on classification patterns. See Section B of the SM for details.

The **Naïve**, **MAR**, and **MNAR** methods each detected a Normal trajectory subgroup (purple) and a Low trajectory subgroup (orange) (SM Figure B.8). Despite similar trajectory patterns across methods, the latent classes appear better separated in the **MNAR** method, particularly for height z-scores for which the response process was modeled. Based on the **MNAR** method, SM Figure B.9 shows that compared to the Low subgroup, the Normal subgroup generally exhibits a higher probability of a clinic visit. Whereas in the Normal subgroup, the probability of a height response is invariably near 1, in the Low subgroup, the response process climbs sharply at the outset. SM Table B.3 presents a summary of posterior latent class assignment under the three methods. The **MNAR** method assigned about 8% fewer children to the Normal subgroup than the other methods. The mean (median) probability of latent class assignment in each subgroup ranged from 0.87 to 0.93 (0.92 to 0.99).

To illustrate patterns of differential child classification by estimation method, we compare the **MAR** versus **MNAR** methods that used all 499 children. SM Table B.4 cross-classifies the 499 children by their latent class assignment from the **MAR** and **MNAR** methods, and the birth weight variable from the latent class membership model. Since few low birth weight (LBW) children were classified differently between the two methods, we focus on the two off-diagonal cells for children born non-LBW. First, 52 non-LBW children were placed in the Normal subgroup by the **MAR** method but the Low subgroup by the **MNAR** method. For height z-scores, the left panel in Figure 2 shows the sample means among the 52 children using their observed measurements, overlaid on the average latent class-specific trajectories estimated by the **MNAR** method. Larger circles indicate sample means with more observed measurements. Sample means with more measurements appear in later follow-up when the latent class-specific trajectories are similar. In fact, the 52 children have few observed measurements in early follow-up when the class trajectories are easily distinguished. In Figure 2, the right panel shows the pattern of the proportions of observed visits in each well-child window among the 52 children, overlaid by the average latent class-specific visit trajectories. Consistent with the **MNAR** method classifying the children in the Low subgroup, the observed visit pattern resembles the Low trajectory.

In the second off-diagonal cell, 17 non-LBW children were placed in the Low subgroup by the **MAR** method but the Normal subgroup by the **MNAR** method (Table B.4). In contrast to the 52 children, the 17 children have more observed height z-scores in early follow-up when the Low and Normal trajectories are easily distinguished (Figure 3, left panel). However, during this period, the observed sample means among the 17 children are located in between the Low and Normal trajectories, rather than showing a clear classification. The **MNAR** method classified the 17 children in the Normal subgroup because their pattern of proportions of observed visits correspond to the visit process trajectory in the Normal subgroup (Figure 3, right panel).

The comparison of the **Naïve** and **MNAR** methods for the 471 common children revealed patterns of classification similar to those heretofore described for the **MAR** and **MNAR** methods (data not shown).

4 Simulation Study

We conducted a simulation study to examine the effect of estimation method on estimating the latent class-specific average health trajectories β_{rk} in (3); and, in predicting a subject’s true latent class assignment. In addition, since scientific inquiry may concern the average health trajectory over time, we considered the effect of estimation method on marginal regression coefficients obtained by averaging β_{rk} over the latent class membership probabilities π_{ik} in (1). For example, for longitudinal health outcome r , the marginal intercept is given by $\tilde{\beta}_{r1} = \frac{1}{n} \sum_{i=1}^n \sum_{k=1}^K \pi_{ik} \beta_{rk1}$. Here, we summarize the design and results, with details in Section C of the SM.

4.1 Design

Based on the real data analysis for $K = 2$ using the **MNAR** method, we generated longitudinal outcomes y_1 and y_2 over 12 time windows for 500 subjects, with about 60% and 40% of subjects in classes 1 and 2, respectively. We assumed an MNAR visit process and response process for y_2 , while y_1 is fully observed given a clinic visit. We then considered five scenarios: S0 is the baseline scenario in which we mimic the latent class-specific average trajectories and missingness proportions in the real data analysis. True parameter values for β_{rk} (3), ϕ_k (5), and λ_{2k} (7) were selected to linearly summarize the estimated trajectories. Latent class 1 is characterized by 55% missed clinic visits and 10% missed y_2 responses. The corresponding values in class 2 are 70% and 20%. SM Figure C.1 depicts S0 for y_1 and y_2 : Corresponding to Figures 2 and 3 in the real data analysis, in early follow-up when the latent class-specific average trajectories are better separated, missingness in y_2 is high in class 2, while in later follow-up, missingness in y_2 is high in class 1.

S1 – S4 make selected changes to S0, as shown in SM Figure C.2 for y_2 . S1 and S2 consider whether the effect of estimation method varies by the degree to which the slopes are different for the latent class-specific average trajectories of y_2 . In S1, we made the slopes more different, while in S2, we made them more similar. S3 and S4 examine whether the effect of estimation method varies by the extent of missingness from the visit and response processes whilst maintaining the shapes of their latent class-specific average trajectories. In S3, we reduced the percent of missed clinic visits to 35% in class 1 and 55% in class 2. In S4, we increased the percent of missed y_2 responses to 25% and 35% in classes 1 and 2, respectively.

For S0–S4, we compare estimation using the **MNAR** method to the **MAR** and **Naïve** methods, based on $K = 2$. For a benchmark, we also include the **Full** method, in which the complete-data model is fit to the full data before introducing any missed visits or responses. We ran 500 data simulations. For β_{rk} and the marginal effects, we examined bias, mean squared error (MSE), 95% coverage probability, and the average length of the 95% credible interval. For subject classification, we considered summary statistics of the proportion of misclassified subjects in each simulation.

4.2 Results

Table 1 shows S0 results. Estimation under the **Full** method presents the benchmark. For the latent class-specific parameters, compared to the **Naïve** and **MAR** methods, the **MNAR** method largely exhibits the smallest bias, the smallest MSE, coverage probability nearest to the nominal level, and the shortest interval length. For example, for y_2 , while the slope in latent class 2, β_{222} , is estimated with negative bias and poor coverage using the **Naïve** and **MAR** methods, bias and coverage under the **MNAR** method are comparable to the **Full** method. The subpar performance of the **Naïve** and **MAR** methods appears to be driven by subject misclassification from class 1 to 2. With respect to the marginal effects, the **MNAR** method again outperforms the **Naïve** and **MAR** methods, demonstrating the smallest bias and MSE and highest coverage probability. However, coverage falls below the nominal level, ranging from 0.89 to 0.93. Even though the **Naïve** and **MAR** methods show shorter interval length than the **MNAR** method, their coverage probabilities are markedly lower.

Full simulation results for S1–S4 are provided in SM Tables C.1–C.4. The performance of the **Full** and **MNAR** methods is robust to these different data generation scenarios. Figure 4 highlights how bias changes by each data generation scenario and estimation method for y_2 . Overall, the **MNAR** method outperforms the **Naïve** and **MAR** methods. In terms of the latent class-specific parameters, while the **MNAR** method performs on par with the **Full** method, using the **Naïve** and **MAR** methods, the degree of bias is contingent on the specific scenario and parameter. For example, for the intercept in class 1 (β_{211}) and the slope in class 2 (β_{222}), bias under the **Naïve** and **MAR** methods decreases when the slopes are more different (S1) versus less different (S2). For all class-specific parameters, bias decreases when visit process missingness is reduced (S3), and bias increases when response process missingness given a clinic visit is

Table 1: Simulation results of S0 for parameter estimation of intercept β_{rk1} and slope β_{rk2} for longitudinal outcome r in latent class k , along with the corresponding marginal intercept and slope, $\tilde{\beta}_{r1}$ and $\tilde{\beta}_{r2}$, respectively, under the **Full**, **Naïve**, **MAR**, and **MNAR** methods. The **Full** method is the benchmark. The best performing method among the **Naïve**, **MAR**, and **MNAR** methods is in bold.

Outcome	Parameter	Method	Truth	Bias	MSE	Coverage	Length
y_1	β_{111} (Class 1 Intercept)	Full	-0.250	-0.002	0.002	0.950	0.190
		Naïve		0.029	0.005	0.904	0.224
		MAR		0.019	0.004	0.908	0.219
		MNAR		0.002	0.003	0.942	0.209
	β_{121} (Class 2 Intercept)	Full	-1.000	0.000	0.003	0.956	0.230
		Naïve		0.046	0.016	0.878	0.404
		MAR		0.004	0.011	0.932	0.370
	β_{112} (Class 1 Slope)	Full	0.100	-0.000	0.000	0.930	0.048
		Naïve		-0.011	0.001	0.928	0.099
		MAR		-0.008	0.001	0.926	0.094
		MNAR		-0.000	0.001	0.954	0.091
	β_{122} (Class 2 Slope)	Full	0.500	0.001	0.001	0.930	0.096
Naïve		-0.089		0.013	0.720	0.266	
MAR		-0.041		0.007	0.850	0.238	
MNAR		-0.001		0.003	0.948	0.215	
y_2	β_{211} (Class 1 Intercept)	Full	0.500	-0.000	0.002	0.954	0.189
		Naïve		0.045	0.006	0.858	0.224
		MAR		0.036	0.005	0.886	0.221
		MNAR		0.005	0.003	0.938	0.210
	β_{221} (Class 2 Intercept)	Full	-0.500	-0.003	0.003	0.940	0.196
		Naïve		0.048	0.015	0.896	0.379
		MAR		0.026	0.011	0.922	0.366
		MNAR		0.000	0.007	0.956	0.310
	β_{212} (Class 1 Slope)	Full	0.200	-0.001	0.000	0.918	0.048
		Naïve		-0.015	0.001	0.904	0.098
		MAR		-0.014	0.001	0.880	0.096
		MNAR		-0.000	0.001	0.950	0.093
β_{222} (Class 2 Slope)	Full	0.750	0.001	0.001	0.934	0.097	
	Naïve		-0.102	0.017	0.646	0.270	
	MAR		-0.075	0.012	0.738	0.262	
	MNAR		-0.003	0.004	0.944	0.237	
y_1	$\tilde{\beta}_{11}$ (Marginal Intercept)	Full	-0.582	-0.001	0.001	0.950	0.147
		Naïve		0.082	0.009	0.574	0.182
		MAR		0.053	0.005	0.774	0.176
		MNAR		0.017	0.003	0.896	0.176
	$\tilde{\beta}_{12}$ (Marginal Slope)	Full	0.277	0.000	0.000	0.952	0.051
		Naïve		-0.065	0.005	0.364	0.109
		MAR		-0.043	0.003	0.610	0.101
		MNAR		-0.008	0.001	0.926	0.104
	$\tilde{\beta}_{21}$ (Marginal Intercept)	Full	0.057	-0.001	0.001	0.954	0.138
		Naïve		0.107	0.014	0.364	0.176
		MAR		0.085	0.010	0.492	0.176
		MNAR		0.021	0.003	0.886	0.177
$\tilde{\beta}_{22}$ (Marginal Slope)	Full	0.444	-0.000	0.000	0.944	0.053	
	Naïve		-0.082	0.008	0.188	0.109	
	MAR		-0.067	0.006	0.350	0.108	
	MNAR		-0.011	0.001	0.918	0.113	

increased (S4). With respect to the marginal effects, bias under the **Naïve** and **MAR** methods is smaller in S2 and S3 compared to the other scenarios. The corresponding bias comparison for y_1 in SM Figure C.3 shows similar patterns of results.

In SM Table C.5, summary statistics of subject misclassification, including the 25th, median, and 75th percentiles, and the minimum and maximum, invariably show the advantage of the **MNAR** method compared to the **Naïve** and **MAR** methods across the data generation scenarios. For example, in S0, the **Full** and **MNAR** methods demonstrated

a median proportion of subjects who are misclassified of 0.02 and 0.03, respectively, whereas the misclassification proportion was 0.15 using the **Naïve** method and 0.14 using the **MAR** method.

5 Discussion

In this study, we developed a Bayesian shared parameter model for multiple longitudinal health outcomes in EHRs to account for a nonignorable visit process and response process given a clinic visit. Our proposed model targets multiple longitudinal health outcomes collected according to a clinically prescribed visit schedule. To account for underlying heterogeneity in EHR patient populations, we used a discrete latent class variable to link GMMs of the longitudinal health outcomes, the visit process, and the response process of individual health outcomes. The use of the discrete latent class variable allowed us to relax the assumption of a single, homogeneous patient population while tractably summarizing innumerable patterns of missingness from the visit and response processes into a small number of latent classes. Particularly important to EHR-based clinical research, we can easily modify our proposed Bayesian shared parameter model in order to conduct a sensitivity analysis about MAR versus MNAR missing data mechanisms for either or both the visit process and the response process given a clinic visit. Example code for model fitting, selection, and checking with our user-friendly R package `EHRmiss` is in Section D of the SM.

Our proposed Bayesian shared parameter model used a discrete latent class variable, targeted multiple longitudinal health outcomes, and distinguished between the visit process and the response process of individual health outcomes. In contrast, in a large clinical database, McCulloch et al. [2016] proposed a shared parameter model for a univariate longitudinal health outcome. The authors defined a single missing data process – which they call the visit process – as a binary indicator for whether a response on the longitudinal health outcome was observed at given time (corresponding to our definition of the response process given a clinic visit). Patient-specific random effects are used as the shared parameter. Notwithstanding their different modeling framework, McCulloch et al. [2016] show analytically that in the absence of accounting for an informative visit process, estimators of regression coefficients associated with the random effects can be badly biased. In our data simulations, we show that failure to account for a nonignorable visit process and response process given a clinic visit may result in biased estimation of latent class-specific average health trajectories, depending on whether the latent classes are well-identified. Identification of the latent classes depends on the extent to which the latent class-specific average health trajectories are different, and the extent to which the degree of missingness permits correctly classifying patients based on their observed longitudinal health outcomes. Even when estimated latent class-specific average health trajectories are largely unbiased, the marginal regression coefficients, which depend on both the class-specific trajectories and the latent class membership probabilities π_{ik} , may be poorly estimated.

In our data application, the assumption of latent heterogeneity in weight and height z-scores, the visit process, and the response process for height z-scores given a clinic visit appeared warranted. Through the discrete latent class variable for a child’s latent class membership, the visit process and the response process for height z-scores informed parameter estimation in the longitudinal model of weight and height z-scores. The role of the visit and response processes was especially evident in the two scenarios depicted by our data application. In the first scenario (Figure 2), a child did not have observed height z-scores during early follow-up when the latent class-specific average height z-score trajectories were easily distinguishable. In the second scenario, a child had observed z-scores during this period of follow-up, but they did not suggest a clear latent classification despite the well-separated latent class-specific average trajectories (Figure 3). In both scenarios, the proposed Bayesian shared parameter model used a child’s patterns of observed visits and responses for height z-scores to help predict latent class membership.

We are primarily interested in two areas for future research. In this work, we were motivated by longitudinal health outcomes in EHRs with a clinically prescribed visit schedule, which we used to discretize time into observation windows during which to measure the visit process and response process given a clinic visit. However, when a prescribed visit schedule is unavailable, measuring the visit process in continuous time is consistent with the data generation in EHRs, since a patient can show up for a clinic visit at any time. We are currently modifying the proposed model to handle continuous time. Second, Bayesian methods can be especially time intensive as the number of observations grows. To enhance the practicality of our proposed model for EHR-based research, we are interested in pursuing strategies for scaling MCMC algorithms to large datasets.

EHRs are increasingly used for applied biomedical research. Rigorous treatment of the two patient-led missing data processes in EHRs, namely, the visit process and the response process of individual health outcomes given a clinic visit, may help to validate clinical findings and to stratify patient risk profiles. The proposed Bayesian shared parameter model for EHRs can be used to evaluate missing data assumptions in scientific inquiries about discovering clinically meaningful subpopulations or population-averaged associations of longitudinal health outcomes with an exposure of interest. Information contained in each patient’s visit and response processes may be valuable for allocating resources

towards at-risk patient subgroups that would benefit from increased monitoring in a health care setting. Our proposed model may be applicable to other routinely collected data sources, like medical claims data.

6 Software

To conduct model fitting, selection, and checking, we built the user-friendly R package EHRMiss available at <https://github.com/anthopolos/EHRMiss>. Example code for analysis with EHRMiss is in Section D in the SM.

7 Supplementary Material

The reader is referred to the on-line Supplementary Materials for explication of the MCMC algorithm for the proposed Bayesian shared parameter model; an addendum to the data application in early childhood weight and height measurements; explication of the simulation study design with additional results; and demonstration of the R package EHRMiss.

Acknowledgments

Ying Wei was supported by NIH grant R01HG008980 and NSF grant DMS-1953527. Qixuan Chen was supported by NIH grant R21ES029668. *Conflict of Interest*: None declared.

References

- J. Albert and S. Chib. Bayesian Analysis of Binary and Polychotomous Response Data. *Journal of the American Statistical Association*, 88(422):669–679, 1993.
- American Academy of Pediatrics. AAP Schedule of Well-Child Care Visits, 2018. URL <https://www.healthychildren.org/English/family-life/health-management/Pages/Well-Child-Care-A-Check-Up-for-Success.aspx>.
- G. Celeux, F. Forbes, C. P. Robert, and D. M. Titterton. Deviance Information Criteria for Missing Data Models. *Bayesian Analysis*, 1(4):651–674, 2006.
- Centers for Disease Control and Prevention. A SAS Program for the 2000 CDC Growth Charts (ages 0 to <20 years), 2019. URL <https://www.cdc.gov/nccdphp/dnpao/growthcharts/resources/sas.htm>.
- M. J. Daniels and J. W. Hogan. *Missing Data in Longitudinal Studies: Strategies for Bayesian Modeling and Sensitivity Analysis*. Chapman and Hall/CRC, Boca Raton, 2008.
- M. R. Elliott, J. J. Gallo, T. R. Ten Have, H. R. Bogner, and I. R. Katz. Using a Bayesian Latent Growth Curve Model to Identify Trajectories of Positive Affect and Negative Events Following Myocardial Infarction. *Biostatistics*, 6(1): 119–143, 2005.
- D. Follmann and M. Wu. An Approximate Generalized Linear Model with Random Effects for Informative Missing Data. *Biometrics*, 51(1):151–168, 1995.
- S. Fruhwirth-Schnatter. *Finite Mixture and Markov Switching Models*. Springer Science & Business Media, New York, 2006.
- E. S. Garrett and S. L. Zeger. Latent Class Model Diagnosis. *Biometrics*, 56:1055–1067, 2000.
- S. Geisser and W. F. Eddy. A Predictive Approach to Model Selection. *Journal of the American Statistical Association*, 74:153–160, 1979.
- A. E. Gelfand and D. K. Dey. Bayesian Model Choice: Asymptotics and Exact Calculations. *Journal of the Royal Statistical Society. Series B (Methodological)*, 56(3):501–514, 1994.
- A. Gelman, I. V. Mechelen, G. Verbeke, D. F. Heitjan, and M. Meulders. Multiple Imputation for Model Checking: Completed-Data Plots with Missing and Latent Data. *Biometrics*, 61:74–85, 2005.
- A. Gelman, J. B. Carlin, H. S. Stern, and D. B. Rubin. *Bayesian Data Analysis*, volume 2. Taylor & Francis, 2014.
- G. Hripcsak and D. J. Albers. Next-Generation Phenotyping of Electronic Health Records. *Journal of the American Medical Informatics Association*, 20(1):117–121, 2013.
- J. G. Ibrahim, M. Chen, and D. Sinha. Model Comparison. In *Bayesian Survival Analysis*, pages 208–261. Springer Science Business Media, LLC, New York, 2001.

- N. M. Laird and J. H. Ware. Random-Effects Models for Longitudinal Data. *Biometrics*, 38(4):963–974, 1982.
- Y. Liang, W. Lu, and Z. Ying. Joint Modeling and Analysis of Longitudinal Data with Informative Observation Times. *Biometrics*, 65:377–384, 2009.
- H. Lin, C. E. McCulloch, and R. A. Rosenheck. Latent Pattern Mixture Models for Informative Intermittent Missing Data in Longitudinal Studies. *Biometrics*, 60(2):295–305, 2004.
- C. E. McCulloch, J. M. Neuhaus, and R. L. Olin. Biased and Unbiased Estimation in Longitudinal Studies with Informative Visit Processes. *Biometrics*, 72(4):1315–1324, 2016.
- B. Muthen, C. H. Brown, K. Masyn, B. Jo, S. Khoo, C. Yang, C. Wang, S. G. Kellam, J. B. Carlin, and J. Liao. General Growth Mixture Modeling for Randomized Preventive Interventions. *Biostatistics*, 3(4):459–475, 2002.
- B. Neelon, G. K. Swamy, L. F. Burgette, and M. L. Miranda. A Bayesian Growth Mixture Model to Examine Maternal Hypertension and Birth Outcomes. *Statistics in Medicine*, 30(22):2721–2735, 2011.
- P. Papastamoulis. label.switching: An r package for dealing with the label switching problem in mcmc outputs. *Journal of Statistical Software*, 69(c01), 2016.
- M. Sanderson, C. Scott, and J. F. Gonzalez. 1988 National Maternal and Infant Health Survey: Methods and Response Characteristics. *Vital and Health Statistics*, 2(125):1–48, 1988.
- G. Schwarz. Estimating the Dimension of a Model. *The Annals of Statistics*, 6(2):461–464, 1978.
- D. J. Spiegelhalter, N. G. Best, B. P. Carlin, and A. Linde. Bayesian Measures of Model Complexity and Fit. *Journal of the Royal Statistical Society, B Methodology*, 64(4):583–639, 2002.
- StataCorp. mprobit – Multinomial Probit Regression. In *Stata 16 Base Reference Manual*, pages 1626–1632. Stata Press, College Station, TX, 2019.
- M. Stephens. Dealing with label switching in mixture models. *Journal of the Royal Statistical Society, B Methodology*, 62(4):795–809, 2000.
- Jianguo Sun, Liuquan Sun, and Dandan Liu. Regression Analysis of Longitudinal Data in the Presence of Informative Observation and Censoring Times. *Journal of the American Statistical Association*, 102(480):1397–1406, 2007.
- G. Verbeke and E. Lesaffre. A Linear Mixed-Effects Model with Heterogeneity in the Random-Effects Population. *Journal of the American Statistical Association*, 91(433):217–221, 1996.
- M. C. Wu and R. J. Carroll. Estimation and Comparison of Changes in the Presence of Informative Right Censoring by Modeling the Censoring Process. *Biometrics*, 44(1):175–188, 1988.

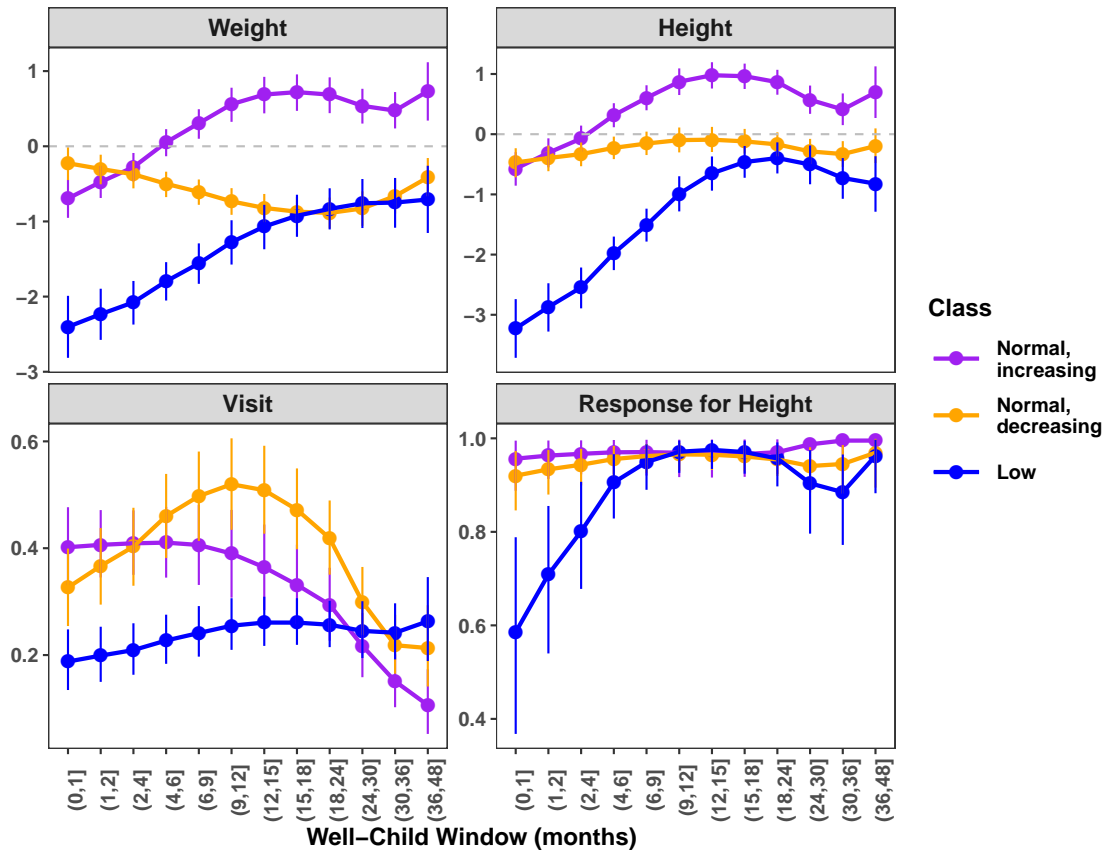


Figure 1: Latent class-specific average trajectories of weight and height z-scores, the probability of a clinic visit, and the probability of a response for height z-scores, estimated by the **MNAR** method.

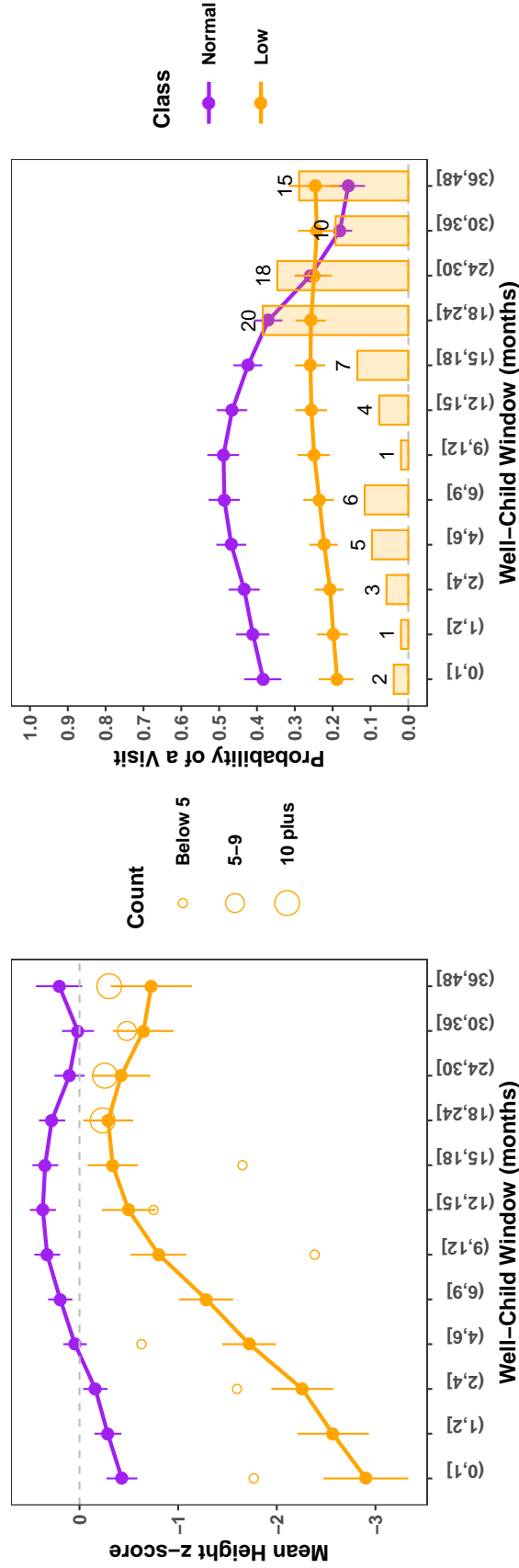


Figure 2: Characterizing the 52 non-low birth weight children classified into the Low trajectory subgroup in the MNAR method but into the Normal trajectory subgroup in the MAR method, assuming 2 latent classes. The left panel shows the sample means of observed height z-scores (hollow circles) in each well-child window, with the circle size indicating the number of measurements. The right panel shows a bar plot of the observed proportions of children with a clinic visit. The count of children with an observed visit in each window is appended. In each panel, corresponding average latent class-specific trajectories estimated with the MNAR method are overlaid.

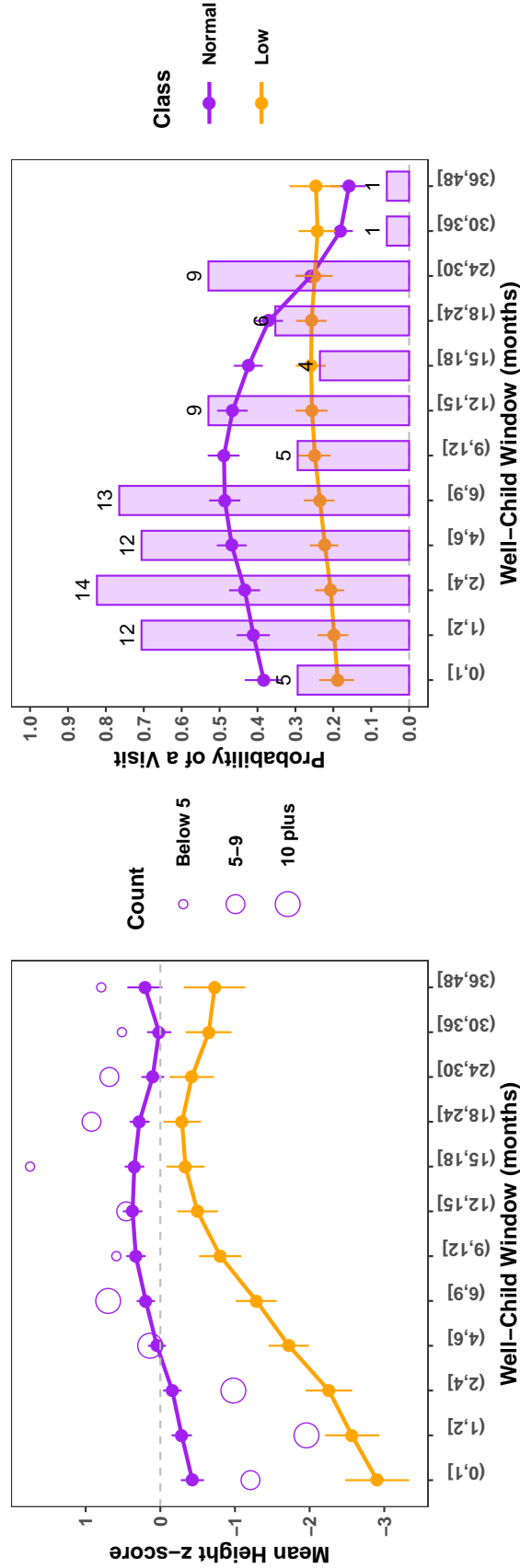


Figure 3: Characterizing the 17 non-low birth weight children classified into the Normal trajectory subgroup in the MNAR method but into the Low trajectory subgroup in the MAR method, assuming 2 latent classes. The left panel shows sample means of observed height z-scores (hollow circles) in each well-child window, with the circle size indicating the number of measurements. The right panel shows a bar plot of the observed proportions of children with a clinic visit. The count of children with an observed visit in each window is appended. In each panel, corresponding average latent class-specific trajectories estimated with the MNAR method are overlaid.

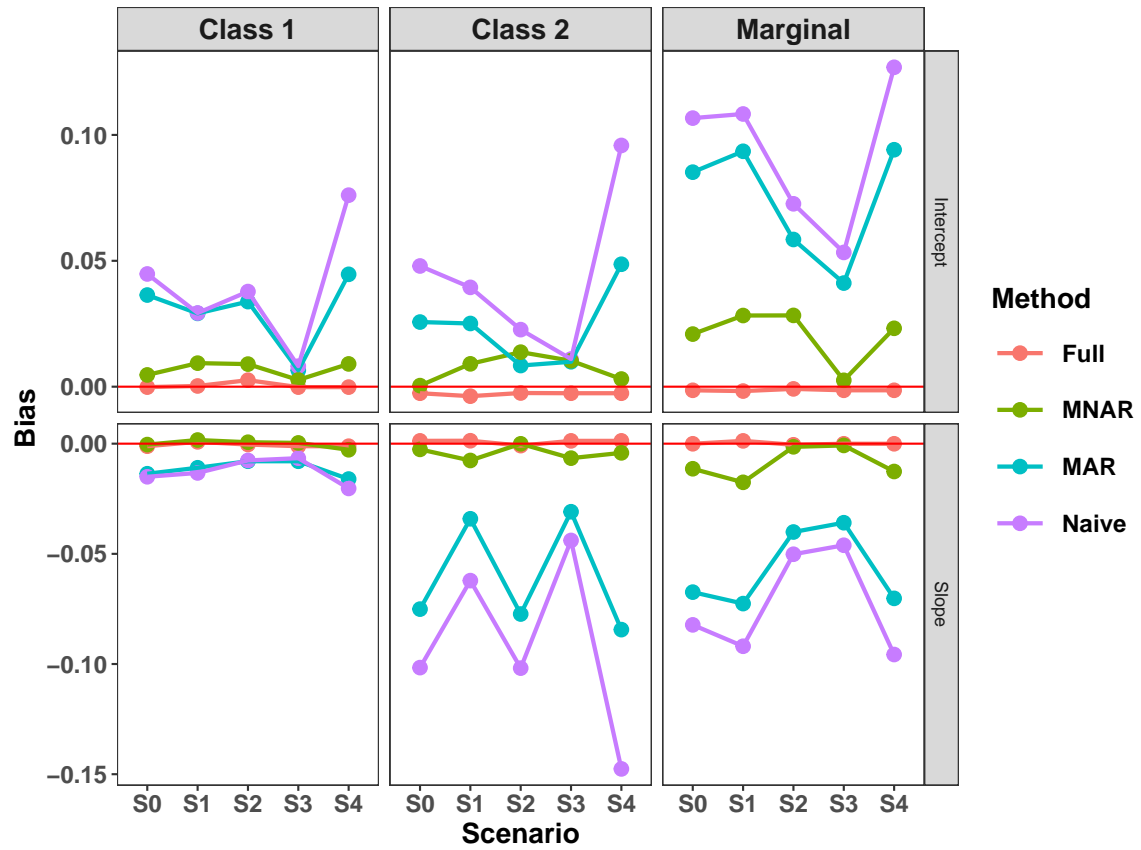


Figure 4: Comparison of bias in parameter estimation for y_2 across data generation scenarios, by estimation method.

“Modeling Heterogeneity and Missing Data of Multiple Longitudinal Outcomes in Electronic Health Records”

Supplementary Materials

Rebecca Anthopolos, Ying Wei, and Qixuan Chen

March 23, 2021

A MCMC Algorithm

We explicate the MCMC algorithm for fitting the proposed shared parameter model to EHRs. In the main text, for ease of model explication, we presented a non-centered parametrization by specifying the random effects \mathbf{b}_{ri} in the longitudinal health outcome model with mean zero. However, in our R package `EHRMiss` available at <https://github.com/anthopolos/EHRMiss>, we used a parametrization based on hierarchical centering in the longitudinal health outcomes model in order to improve chain mixing and speed model convergence [Gelfand et al., 1995, 1996]. In the hierarchically centered parametrization, we centered \mathbf{b}_{ri} around the average health trajectory represented by β_{rk} . The MCMC algorithm herein is based on this hierarchically centered parametrization given by

$$\left[\begin{array}{c} \mathbf{y}_{1i} \\ \vdots \\ \mathbf{y}_{Ri} \end{array} \middle| c_i = k \right] \sim MVN_{RJ} \left(\begin{array}{c} \beta_{1k} \mathbf{x}_i^{h,T} + \mathbf{b}_{1i} \mathbf{z}_i^T \\ \vdots \\ \beta_{Rk} \mathbf{x}_i^{h,T} + \mathbf{b}_{Ri} \mathbf{z}_i^T \end{array}, \text{diag}(\boldsymbol{\Sigma}_k) \right) \quad (1)$$

$$\left[\begin{array}{c} \mathbf{b}_{1i} \\ \vdots \\ \mathbf{b}_{Ri} \end{array} \middle| c_i = k \right] \sim MVN_{Rq} \left(\begin{array}{c} \mathbf{u}_i \eta_{1k}^T \\ \vdots \\ \mathbf{u}_i \eta_{Rk}^T \end{array}, \boldsymbol{\Psi}_k \right) \quad (2)$$

where we use a superscript h for the fixed effects design matrix \mathbf{x}_i^h ($J \times p^h$) to indicate the change in parameterization. Unlike the main text, in (1), the columns in the random effects design matrix \mathbf{z}_i are no longer a subset of the columns in \mathbf{x}_i^h . For example, in a random intercept model, only \mathbf{z}_i will include a column of ones for an intercept. In (2), the random effects $\mathbf{b}_{1i}, \dots, \mathbf{b}_{Ri}$ are distributed with mean as a function of patient-level risk factors in \mathbf{u}_i ($1 \times e$) and corresponding regression coefficients in $\eta_{1k}, \dots, \eta_{Rk}$ ($q \times e$). $\text{diag}(\boldsymbol{\Sigma}_k)$ is an $RJ \times RJ$ block diagonal matrix with elements $\boldsymbol{\Sigma}_k$ for the variance-covariance among y_{1ij}, \dots, y_{Rij} in each time window j ($j = 1, \dots, J$).

A.1 Update parameters in the latent class membership model

The Gibbs steps are given for the latent class membership model.

1. Update ξ_{ik} . Let $\xi_i^T = (\xi_{i1}, \dots, \xi_{iK-1})$ be a $(K-1)$ -length column vector. Per McCulloch and Rossi [1994], for $i = 1, \dots, n$, the distribution of $\xi_i \mid \delta, c_i$ is a $(K-1)$ -variate normal distribution truncated over the appropriate cone in \mathbf{R}^{K-1} . Let \mathbf{c}_i^* be a multinomial vector with entries $\mathbf{c}_i^* = (c_{i1}^*, \dots, c_{iK}^*)$ equal to 1 if the i^{th} subject is in latent class k and 0 otherwise. If $c_{ik}^* = 1$, then $\xi_{ik} > \max(\xi_{i,-k}, 0)$. If $c_{ik}^* = 0$, then $\xi_{ik} < \max(\xi_{i,-k}, 0)$. $\xi_{i,-k}$ is a $K-2$ dimensional vector of all components of ξ_i excluding ξ_{ik} . This algorithm avoids the problem of drawing from a truncated multivariate normal. Instead each draw is a truncated univariate normal because we are using the conditional distribution $\xi_{ik} \mid \xi_{i,-k}, \delta_k, c_i$, where $c_i = K$ if $\max(\xi_i) < 0$, or else $c_i = \text{index of } \max(\xi_i)$ for $k = 1, \dots, K-1$.
2. Update δ_k . For $k = 1, \dots, K-1$, we assume the prior $\delta_k \sim MVN_s(0, \boldsymbol{\Sigma}_\delta)$. The full conditional is $MVN_s(\mu_{\delta_k}, \mathbf{V}_\delta)$, where

$$\mathbf{V}_\delta = \left(\sum_{i=1}^n \mathbf{w}_i^T \mathbf{w}_i + \boldsymbol{\Sigma}_\delta^{-1} \right)^{-1}$$

$$\mu_{\delta_k} = \mathbf{V}_\delta \times \left(\sum_{i=1}^n \mathbf{w}_i^T \xi_{ik} \right),$$

with \mathbf{w}_i being an s -length row vector of patient-level risk factors, including a column of ones for an intercept.

A.2 Update parameters in the longitudinal outcomes model

1. Update β_{rk} .

To update β_{rk} , based on the properties of the multivariate normal distribution, we use the conditional distribution of longitudinal health outcome r given health outcomes r' for all $r' \neq r$. Let $\mathbf{y}_{ri}^* = (y_{riA(1)}, \dots, y_{riA(n_i)})^T$. Let \mathbf{Q} be a matrix of conditional coefficients defined as $\mathbf{Q} = \mathbf{I} - [\text{diag}(\boldsymbol{\Sigma}_k^{-1})]^{-1} \boldsymbol{\Sigma}_k^{-1}$, with elements $q_{rr'}$ ($r = 1, \dots, R$, $r' = 1, \dots, R$) [Gelman et al., 2014]. For longitudinal health outcome r of patient i in window j , the conditional distribution of \mathbf{y}_{ri}^* given $\mathbf{y}_{r'i}^*$ for all $r' \neq r$ and latent class c_i is

$$\begin{aligned} & [\mathbf{y}_{ri}^* | \mathbf{y}_{r'i}^*, \text{ all } r' \neq r, c_i = k] \sim \\ & MVN_{n_i} \left(\beta_{rk} \mathbf{x}_i^{h*,T} + \mathbf{b}_{ri} \mathbf{z}_i^{*,T} + \sum_{r' \neq r} q_{rr'} (\mathbf{y}_{r'i}^* - \beta_{r'k} \mathbf{x}_i^{h*,T} - \mathbf{b}_{r'i} \mathbf{z}_i^{*,T}), \text{diag}([\boldsymbol{\Sigma}_{krr}^{-1}]^{-1}) \right), \end{aligned} \quad (3)$$

where \mathbf{x}_i^{h*} ($n_i \times p^h$) is the fixed effects design matrix for time windows $A(l)$ for $l = 1, \dots, n_i$. \mathbf{z}_i^* is the corresponding random effects design matrix.

For latent classes $k = 1, \dots, K$, assuming the prior distribution $\beta_{rk} \sim MVN_{p^h}(\mathbf{0}, \boldsymbol{\Sigma}_\beta)$, the full conditional is $MVN_{p^h}(\mu_{\beta_{rk}}, \mathbf{V}_{\beta_{rk}})$, where

$$\mathbf{V}_{\beta_{rk}} = \left(\sum_{i=1}^n \mathbf{1}_{c_i=k} \times \frac{\mathbf{x}_i^{h*,T} \mathbf{x}_i^{h*}}{[\boldsymbol{\Sigma}_{krr}^{-1}]^{-1}} + \boldsymbol{\Sigma}_\beta^{-1} \right)^{-1}$$

$\mu_{\beta_{rk}}$

$$\begin{aligned} & = \mathbf{V}_{\beta_{rk}} \\ & \times \left(\sum_{i=1}^n \mathbf{1}_{c_i=k} \times \frac{\mathbf{x}_i^{h*,T} \left(\mathbf{y}_{ri}^{*,T} - \mathbf{z}_i^* \mathbf{b}_{ri}^T - (\sum_{r' \neq r} q_{rr'} (\mathbf{y}_{r'i}^* - \beta_{r'k} \mathbf{x}_i^{h*,T} - \mathbf{b}_{r'i} \mathbf{z}_i^{*,T}))^T \right)}{[\boldsymbol{\Sigma}_{krr}^{-1}]^{-1}} \right) \end{aligned}$$

2. Update \mathbf{b}_{ri} . Using the conditional distribution in (3), the full conditional is

$MVN_q(\mu_{b_{ri}}, \mathbf{V}_{b_{ri}})$, where

$$\mathbf{V}_{b_{ri}} = \sum_{k=1}^K \mathbf{1}_{c_i=k} \left(\frac{\mathbf{z}_i^{*,T} \mathbf{z}_i^*}{[\boldsymbol{\Sigma}_{krr}^{-1}]^{-1}} + \boldsymbol{\Psi}_{kr}^{-1} \right)^{-1}$$

$$\begin{aligned}
& \mu_{b_{ri}} \\
&= \mathbf{V}_{b_{ri}} \\
&\times \sum_{k=1}^K \mathbf{1}_{c_i=k} \\
&\times \left(\frac{\mathbf{z}_i^{*,T} \left(\mathbf{y}_{ri}^{*,T} - \mathbf{x}_i^{h*} \beta_{rk}^T - (\sum_{r' \neq r} q_{rr'} (\mathbf{y}_{r'i}^* - \beta_{r'k} \mathbf{x}_i^{h*,T} - \mathbf{b}_{r'i} \mathbf{z}_i^{*,T})) \right)^T}{[\boldsymbol{\Sigma}_{kr}^{-1}]^{-1}} + \boldsymbol{\Psi}_{kr}^{-1} \eta_{rk} \mathbf{u}_i^T \right)
\end{aligned}$$

3. Update η_{rk} . Let the elements of \mathbf{b}_{ri} be indexed as b_{rig} for $g = 1, \dots, q$. For the g^{th} random effect, let $\eta_{rkg} = (\eta_{rkg1}, \dots, \eta_{rkgq})^T$ ($1 \times e$). Then, $b_{rig} \sim N(\mathbf{u}_i \eta_{rkg}^T, \psi_{krkg})$. Assuming the prior distribution $MVN_e(\mathbf{0}, \boldsymbol{\Sigma}_\eta)$, the full conditional of η_{rkg} is $MVN_e(\mu_{\eta_{rkg}}, \mathbf{V}_{\eta_{rkg}})$, where

$$\begin{aligned}
\mathbf{V}_{\eta_{rkg}} &= \left(\sum_{i=1}^n \mathbf{1}_{c_i=k} \times \frac{\mathbf{u}_i^T \mathbf{u}_i}{\psi_{krkg}} + \boldsymbol{\Sigma}_\eta^{-1} \right)^{-1} \\
\mu_{\eta_{rkg}} &= \mathbf{V}_{\eta_{rkg}} \times \left(\sum_{i=1}^n \mathbf{1}_{c_i=k} \times \frac{\mathbf{u}_i^T b_{rig}}{\psi_{krkg}} \right)
\end{aligned}$$

4. Update $\boldsymbol{\Sigma}_k$. Recall the R -length row vectors $\mathbf{y}_{iA(l)} = (y_{1iA(l)}, \dots, y_{RiA(l)})^T$, and $\mu_{iA(l)} = \mathbf{x}_{iA(l)} \beta_k^T + \mathbf{z}_{iA(l)} \mathbf{b}_i^T$. Assuming an inverse-Wishart prior distribution $\boldsymbol{\Sigma}_k \sim IW(\nu_\Sigma, S_\Sigma^{-1})$, the full conditional is $IW(a_{\Sigma_k}, b_{\Sigma_k})$, where

$$\begin{aligned}
a_{\Sigma_k} &= \nu_\Sigma + \sum_{i=1}^n \mathbf{1}_{c_i=k} \times n_i \\
b_{\Sigma_k} &= S_\Sigma + \sum_{i=1}^n \mathbf{1}_{c_i=k} \sum_{l=1}^{n_i} (\mathbf{y}_{iA(l)} - \mu_{iA(l)})^T (\mathbf{y}_{iA(l)} - \mu_{iA(l)})
\end{aligned}$$

5. Update $\boldsymbol{\Psi}_k$. The block diagonal matrix $\boldsymbol{\Psi}_k$ ($Rq \times Rq$) contains elements $\boldsymbol{\Psi}_{kr}$ ($q \times q$). Assuming $\boldsymbol{\Psi}_{kr} \sim IW(\nu_\Psi, S_\Psi^{-1})$, the full conditional is $IW(a_{\Psi_{kr}}, b_{\Psi_{kr}})$, where

$$\begin{aligned}
a_{\Psi_{kr}} &= \nu_\Psi + \sum_{i=1}^n \mathbf{1}_{c_i=k} \\
b_{\Psi_{kr}} &= S_\Psi + \sum_{i=1}^n \mathbf{1}_{c_i=k} \times (\mathbf{b}_{ri} - \mathbf{u}_i \eta_{rk}^T)^T (\mathbf{b}_{ri} - \mathbf{u}_i \eta_{rk}^T)
\end{aligned}$$

A.3 Update parameters in the visit process model

Following Albert and Chib [1993], we use a data augmentation approach [Tanner and Wong, 1987] to model the probability of a clinic visit using Bayesian probit regression. Corresponding to the visit process for patient i in clinical window j , we introduce latent variables ξ_{ij}^d ($i = 1, \dots, n$, $j = 1, \dots, J$). The latent variables ξ_{ij}^d are assumed to be distributed as $N(\mathbf{x}_{ij}\phi_k^T + \mathbf{z}_{ij}\tau_i^T, 1)$, where the observation-level error variance is fixed to 1. To connect latent ξ_{ij}^d to the visit process d_{ij} , define $d_{ij} = 1$ if $\xi_{ij}^d > 0$ and $d_{ij} = 0$ if $\xi_{ij}^d \leq 0$. With the introduction of the latent variables, the Gibbs sampling steps are as follows.

1. Update ξ_{ij}^d . The full conditional is $\xi_{ij}^d | d_{ij}, \phi_k, \tau_i, c_i = k \sim N(\sum_{k=1}^K \mathbf{1}_{c_i=k} \times (\mathbf{x}_{ij}\phi_k^T + \mathbf{z}_{ij}\tau_i^T), 1)$, truncated at the left by 0 if $d_{ij} = 1$. Otherwise, $\xi_{ij}^d | d_{ij}, \phi_k, \tau_i, c_i = k \sim N(\sum_{k=1}^K \mathbf{1}_{c_i=k} \times (\mathbf{x}_{ij}\phi_k^T + \mathbf{z}_{ij}\tau_i^T), 1)$, truncated at the right by 0 if $d_{ij} = 0$.
2. Update ϕ_k . For latent classes $k = 1, \dots, K$, assuming the prior distribution $\phi_k \sim MVN_p(\mu_\phi, \Sigma_\phi)$, the full conditional is $MVN_p(\mu_{\phi_k}, \mathbf{V}_{\phi_k})$, where

$$\mathbf{V}_{\phi_k} = \left(\sum_{i=1}^n \mathbf{1}_{c_i=k} \times \mathbf{x}_i^T \mathbf{x}_i + \Sigma_\phi^{-1} \right)^{-1}$$

$$\mu_{\phi_k} = \mathbf{V}_{\phi_k} \times \left(\sum_{i=1}^n \mathbf{1}_{c_i=k} \times \mathbf{x}_i^T \left(\xi_i^{d,T} - \mathbf{z}_i \tau_i^T \right) + \Sigma_\phi^{-1} \mu_\phi^T \right),$$

where the random effects design matrix \mathbf{z}_i ($J \times q$) contains a subset of the columns in the fixed effects design matrix \mathbf{x}_i ($J \times p$).

3. Update τ_i . The full conditional is $MVN_q(\mu_{\tau_i}, \mathbf{V}_{\tau_i})$, where

$$\mathbf{V}_{\tau_i} = \sum_{k=1}^K \mathbf{1}_{c_i=k} \times \left(\mathbf{z}_i^T \mathbf{z}_i + \Omega_k^{-1} \right)^{-1}$$

$$\mu_{\tau_i} = \mathbf{V}_{\tau_i} \times \sum_{k=1}^K \mathbf{1}_{c_i=k} \times \left(\mathbf{z}_i^T \left(\xi_i^{d,T} - \mathbf{x}_i \phi_k^T \right) \right)$$

4. Update Ω_k . Assuming an inverse-Wishart prior distribution $\Omega_k \sim IW(\nu_\Omega, S_\Omega^{-1})$, the full

conditional is $IW(a_{\Omega_k}, b_{\Omega_k})$, where

$$a_{\Omega_k} = \nu_{\Omega} + \sum_{i=1}^n \mathbf{1}_{c_i=k}$$

$$b_{\Omega_k} = S_{\Omega} + \sum_{i=1}^n \mathbf{1}_{c_i=k} \times \tau_i^T \tau_i$$

A.4 Update parameters in the response process given a clinic visit model

The Gibbs steps to update the parameters in the model for the response process given a clinic visit are analogous to the steps in the visit process model, except that we use observed clinic visits.

For patient i in clinical window l with an observed visit ($l = 1, \dots, n_i$), we introduce latent variables $\xi_{riA(l)}^m$ ($i = 1, \dots, n, l = 1, \dots, n_i$). The latent variables $\xi_{riA(l)}^m$ are assumed to be distributed as $N(\mathbf{x}_{iA(l)} \lambda_{rk}^T + \mathbf{z}_{iA(l)} \kappa_{ri}^T, 1)$, where the observation-level error variance is fixed to 1. To connect latent $\xi_{riA(l)}^m$ to the response process $m_{riA(l)}$, define $m_{riA(l)} = 1$ if $\xi_{riA(l)}^m > 0$ and $m_{riA(l)} = 0$ if $\xi_{riA(l)}^m \leq 0$. Upon introducing the latent variables, the Gibbs sampling steps for λ_{rk} , κ_{ri} , and Θ_{rk} proceed as in the visit process model.

A.5 Update latent class membership

Sample latent class indicators c_i for $i = 1, \dots, n$ from $Multinomial(1; p_{i1}, \dots, p_{iK})$, where p_{i1}, \dots, p_{iK} are the posterior probabilities of latent class assignment. For $k = 1, \dots, K$,

$$p_{ik}$$

$$= Pr(c_i = k | \pi_{ik}; \mathbf{y}_i^*, \mathbf{b}_i; \mathbf{d}_i, \tau_i; \mathbf{m}_{1i}, \dots, \mathbf{m}_{Ri}, \kappa_{1i}, \dots, \kappa_{Ri}; rest)$$

$$\propto \pi_{ik} f(\mathbf{y}_i^* | \mathbf{b}_i, \beta_k, \Sigma_k^*) f(\mathbf{b}_i | \Psi_k)$$

$$\times f(\mathbf{d}_i | \tau_i, \phi_k) f(\tau_i | \Omega_k)$$

$$\times \prod_{r=1}^R f(\mathbf{m}_{ri} | \kappa_{ri}, \lambda_{rk}) f(\kappa_{ri} | \Theta_{rk}),$$

where $\mathbf{y}_i^* = (\mathbf{y}_{iA(1)}^T, \dots, \mathbf{y}_{iA(n_i)}^T)$, and Σ_k^* is an $n_i R \times n_i R$ block diagonal matrix with elements Σ_k ($R \times R$) for each $\mathbf{y}_{iA(l)}$ ($l = 1, \dots, n_i$).

B Analysis of Early Childhood Weight and Height Measurements Addendum

Based on the well-child windows, Figure B.1 presents the patterns of observed visits and responses for weight and height given a clinic visit. Of 5,988 well-child windows (499 children \times 12 well-child windows), 67% correspond to missed visits. Among 1,983 observed visits, only 17 weight measurements are missing ($< 1\%$), whereas 207 height measurements (10%) are missing.

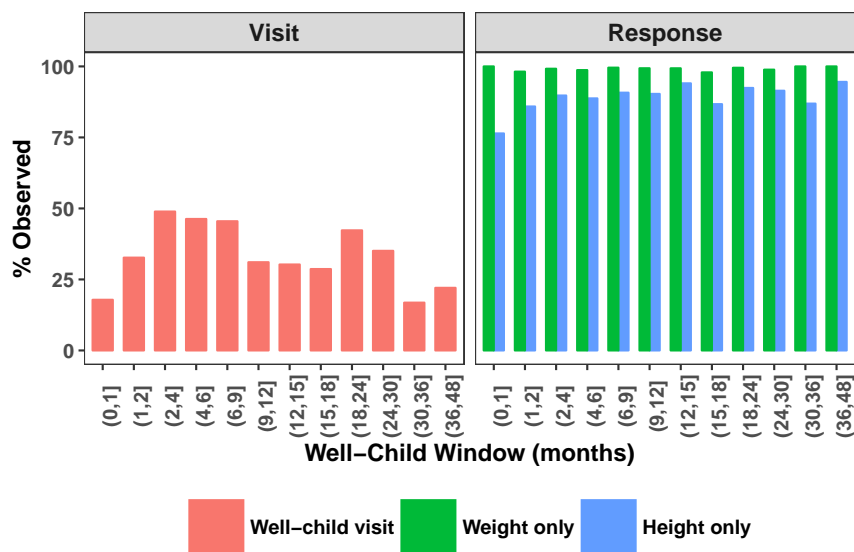


Figure B.1: Patterns of observed visits and observed responses in weight and height z-scores given a clinic visit.

B.1 Longitudinal trajectories of weight and height z-scores using the MNAR method

B.1.1 Model selection

In GMMs, the number of latent classes K is assumed to be fixed and known. A challenge in data applications with GMMs is to select among models with varying numbers of latent classes. We compared $K = 2, 3, 4$ -class models based on the **MNAR** method using model information criteria, including the Bayesian Information Criterion (BIC) [Schwarz, 1978] and a modified version of the Deviance Information Criterion (DIC) [Spiegelhalter et al., 2002] known as the DIC3 recommended for latent variable models [Celeux et al., 2006]; the log-pseudo marginal likelihood (LPML) [Geisser

and Eddy, 1979, Gelfand and Dey, 1994, Ibrahim et al., 2001]; and a graphical technique known as latent class identifiability displays (LCIDs) [Garrett and Zeger, 2000]. To select among models with varying numbers of latent classes, we use two model information criteria, including the Bayesian Information Criterion (BIC) [Schwarz, 1978] and a modified version of the Deviance Information Criterion (DIC) [Spiegelhalter et al., 2002] known as the DIC3 [Celeux et al., 2006], the log-pseudo marginal likelihood [Geisser and Eddy, 1979, Gelfand and Dey, 1994, Ibrahim et al., 2001], and a graphical technique known as latent class identifiability displays (LCIDs) [Garrett and Zeger, 2000]. With the objective of clinical interpretability, we prioritized a solution to the number of latent classes that represented distinctive clusters of children.

We calculate the BIC using the marginal density of \mathbf{y}_i^* , \mathbf{d}_i , $\mathbf{m}_{1i}, \dots, \mathbf{m}_{Ri}$ after integrating out c_i and random effects \mathbf{b}_i , τ_i , and $\kappa_{1i}, \dots, \kappa_{Ri}$, given by

$$\begin{aligned}
& f(\mathbf{y}_i^*, \mathbf{d}_i, \mathbf{m}_{1i}, \dots, \mathbf{m}_{Ri} \mid \pi; \beta, \Sigma, \Psi; \phi, \Omega; \lambda, \Theta) \\
&= \sum_{k=1}^K \pi_{ik} \left(\int_{\mathbf{b}_i} f(\mathbf{y}_i^* \mid \mathbf{b}_i, \beta_k, \Sigma_k^*) f(\mathbf{b}_i \mid \Psi_k) \partial \mathbf{b}_i \right) \\
&\times \left(\int_{\tau_i} f(\mathbf{d}_i \mid \tau_i, \phi_k) f(\tau_i \mid \Omega_k) \partial \tau_i \right) \\
&\times \left(\int_{\kappa_{Ri}} \dots \int_{\kappa_{1i}} f(\mathbf{m}_{1i} \mid \kappa_{1i}, \lambda_{1k}) f(\kappa_{1i} \mid \Theta_{1k}) \dots f(\mathbf{m}_{Ri} \mid \kappa_{Ri}, \lambda_{Rk}) f(\kappa_{Ri} \mid \Theta_{Rk}) \partial \kappa_{1i}, \dots, \partial \kappa_{Ri} \right),
\end{aligned} \tag{4}$$

where we can analytically compute only the integral for \mathbf{y}_i^* , and we estimate the integrals for \mathbf{d}_i and $\mathbf{m}_{1i}, \dots, \mathbf{m}_{Ri}$ using numerical integration. We then define the BIC as

$$\text{BIC} = \sum_{i=1}^n \log f(\mathbf{y}_i^*, \mathbf{d}_i, \mathbf{m}_{1i}, \dots, \mathbf{m}_{Ri} \mid \hat{\pi}; \hat{\beta}, \hat{\Sigma}, \hat{\Psi}; \hat{\phi}, \hat{\Omega}; \hat{\lambda}, \hat{\Theta}) + d \log N_{\text{eff}},$$

where $\hat{\pi}$, $\hat{\beta}$, $\hat{\Sigma}$, $\hat{\Psi}$, $\hat{\phi}$, $\hat{\Omega}$, $\hat{\lambda}$, $\hat{\Theta}$ are the Bayesian estimators of the unknown parameters; d is the number of free parameters; and N_{eff} is the effective sample size from the model of \mathbf{y}_i^* , which we estimate by accounting for correlations among longitudinal measurements from same patient [Jones, 2011]. The first term is a measure of goodness of fit, and the second term provides a penalty for model complexity.

Since the number of free parameters may be unclear in Bayesian hierarchical models, the DIC was proposed [Spiegelhalter et al., 2002] in which the number of effective parameters is estimated as

the difference between the posterior mean deviance and a point estimate of the deviance commonly computed with the posterior mean estimator of unknown parameters. However, because in finite mixture modeling, the posterior mean estimator often leads to a negative effective number of parameters, the DIC3 is instead based on the estimator of the marginal density in (4) [Celeux et al., 2006]. Like the BIC, the DIC3 penalizes goodness of fit by model complexity. Smaller values of BIC and DIC3 indicate a preferred model.

Based on leave-one-out cross-validation, the LPML is a summary measure of a model’s predictive utility, and is calculated as the log of the product of the conditional predictive ordinate (CPO) for each patient under a given model [Geisser and Eddy, 1979, Gelfand and Dey, 1994, Ibrahim et al., 2001]. For patient i , the CPO is the marginal posterior predictive density given that patient i is excluded from the dataset. Using (4), a Monte Carlo estimate of the CPO for patient i is given by

$$\widehat{\text{CPO}}_i = \frac{G}{\sum_{g=1}^G (1/f(\mathbf{y}_i^*, \mathbf{d}_i, \mathbf{m}_{1i}, \dots, \mathbf{m}_{Ri} | \pi^g; \beta^g, \boldsymbol{\Sigma}^g, \boldsymbol{\Psi}^g; \phi^g, \boldsymbol{\Omega}^g; \lambda^g, \boldsymbol{\Theta}^g))},$$

where superscript g indexes parameters sampled over MCMC iterations $g = 1, \dots, G$ following a burn-in period. Then, the LPML is estimated by $\widehat{\text{LPML}} = \sum_{i=1}^n \log \widehat{\text{CPO}}_i$. Larger values of the LPML indicate a preferred model.

Latent class identifiability displays (LCIDs) [Garrett and Zeger, 2000] overlay the prior versus posterior distributions for the regression coefficients δ_k in the latent class membership model: When the prior and posterior distributions are largely overlapping, the number of latent classes may be too large given the data.

In Table B.1, the DIC3 and LPML both chose the 3-class model, whereas the BIC selected the 4-class model. For each of the K -class models, Figures B.2–B.4 show the posterior versus prior distributions for the covariates in the latent class membership model. Compared to the 4-class model, the 3-class model appears to identify distinctive population subgroups according to race, sex, and birth weight. We therefore selected the 3-class model.

Table B.1: Comparison of models with $K = 2, 3, 4$ latent class using the **MNAR** method. A preferred model is indicated by smaller values of the BIC and DIC3 and larger values of the LPML.

Criterion	K		
	2	3	4
BIC	21625	21226	20939
DIC3	23263	22716	22741
LPML	-12770	-12230	-13500

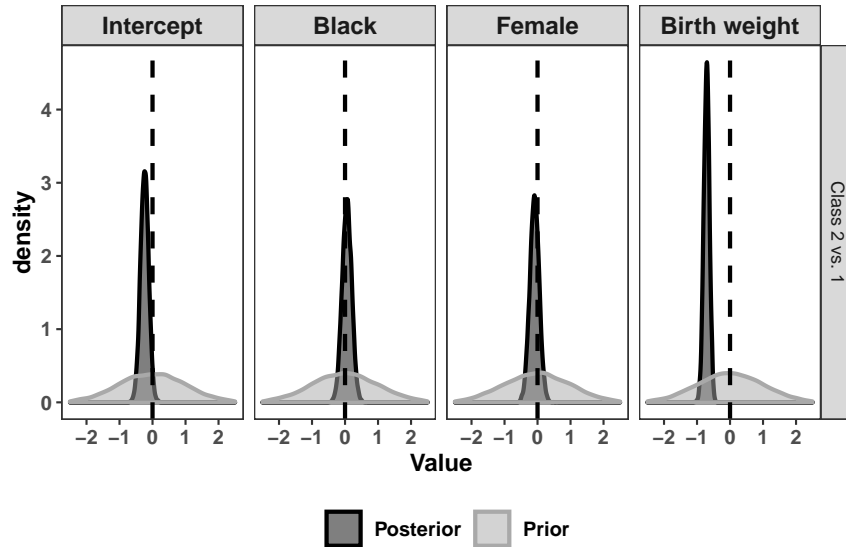


Figure B.2: Posterior versus prior distributions for the covariates in the multinomial probit model of latent class membership using the **MNAR** method, $K = 2$.

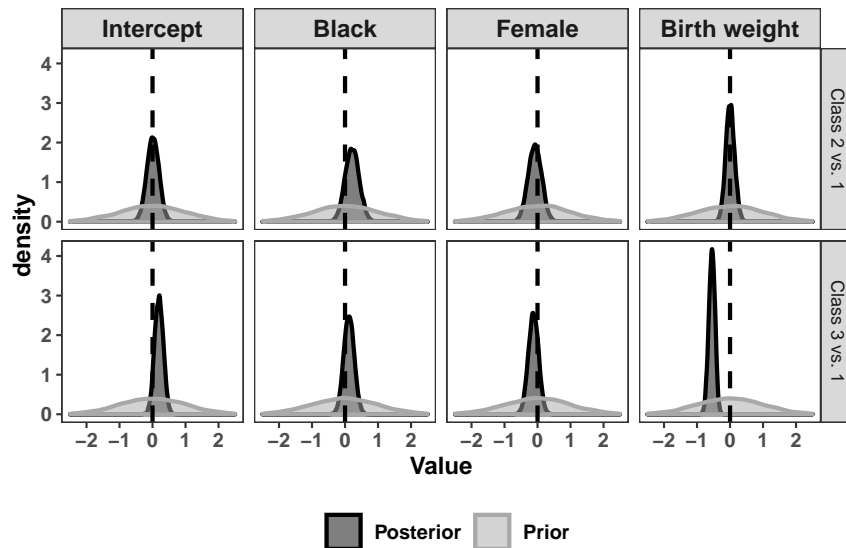


Figure B.3: Posterior versus prior distributions for the covariates in the multinomial probit model of latent class membership using the **MNAR** method, $K = 3$.

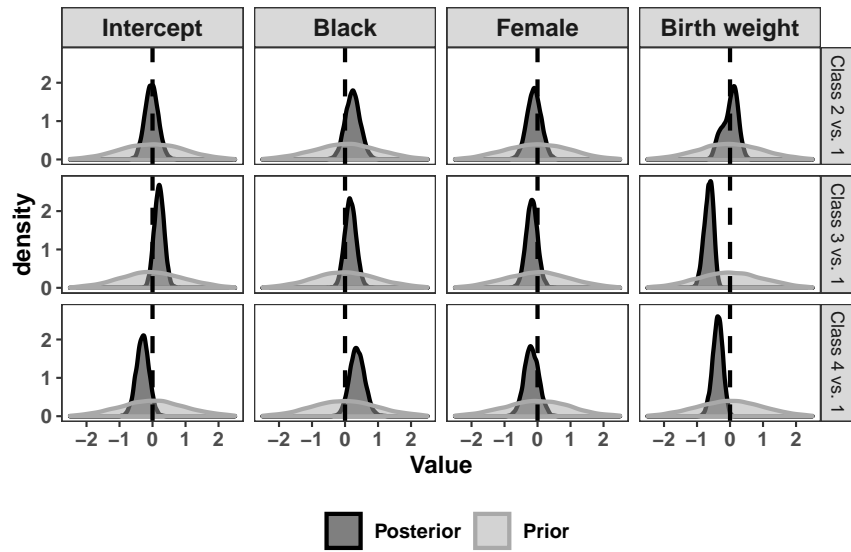


Figure B.4: Posterior versus prior distributions for the covariates in the multinomial probit model of latent class membership using the **MNAR** method, $K = 4$.

B.1.2 The 3-class model using the MNAR method

Based on the maximum of a child’s mean posterior probabilities of belonging to each latent class, we assigned approximately one-third of children to each subgroup, with subgroup mean (median) probability ranging from 0.81 to 0.84 (0.84 to 0.93) (Table B.2).

Table B.2: Posterior latent class assignment in the 3-class model using the **MNAR** method. Children were assigned to the Normal, increasing; Normal, decreasing; or Low trajectory subgroups according to the maximum of the mean posterior probabilities of class assignment.

	Normal, increasing	Normal, decreasing	Low
Predicted class size (%)	162 (32)	160 (32)	177 (35)
Mean probability	0.81	0.84	0.84
Median probability	0.84	0.93	0.93

Comparison of the completed datasets that include observed and imputed weight and height z-scores in each well-child window, and replicates of the completed datasets drawn from the posterior predictive distribution demonstrated adequate model fit. Figure B.5 presents a scatter plot of the discrepancy measure T across MCMC samples, with the horizontal and vertical axes being T based on the completed and replicated datasets, respectively. Comparing completed and replicated T , the Bayesian predictive p-value of 0.44 suggests adequate overall model fit. In addition, we compared histograms of randomly selected completed and replicated datasets of weight and height z-scores. In Figures B.6 and B.7, the distribution of z-scores by subgroup and well-child window appears largely consistent between the completed and replicated datasets.

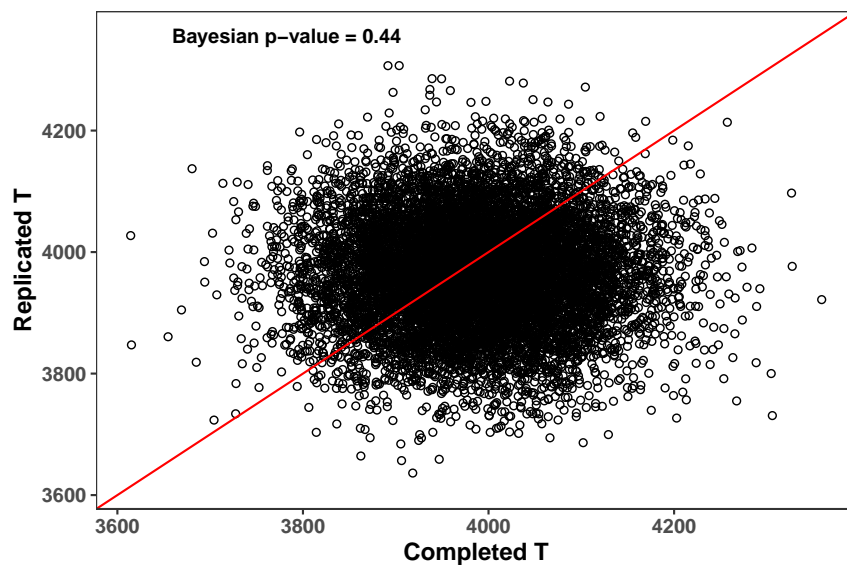


Figure B.5: Posterior predictive checking for the 3-class model estimated using the **MNAR** method. Completed T is computed using the completed data. Replicated T is computed using the replicated completed datasets from the posterior predictive distribution.

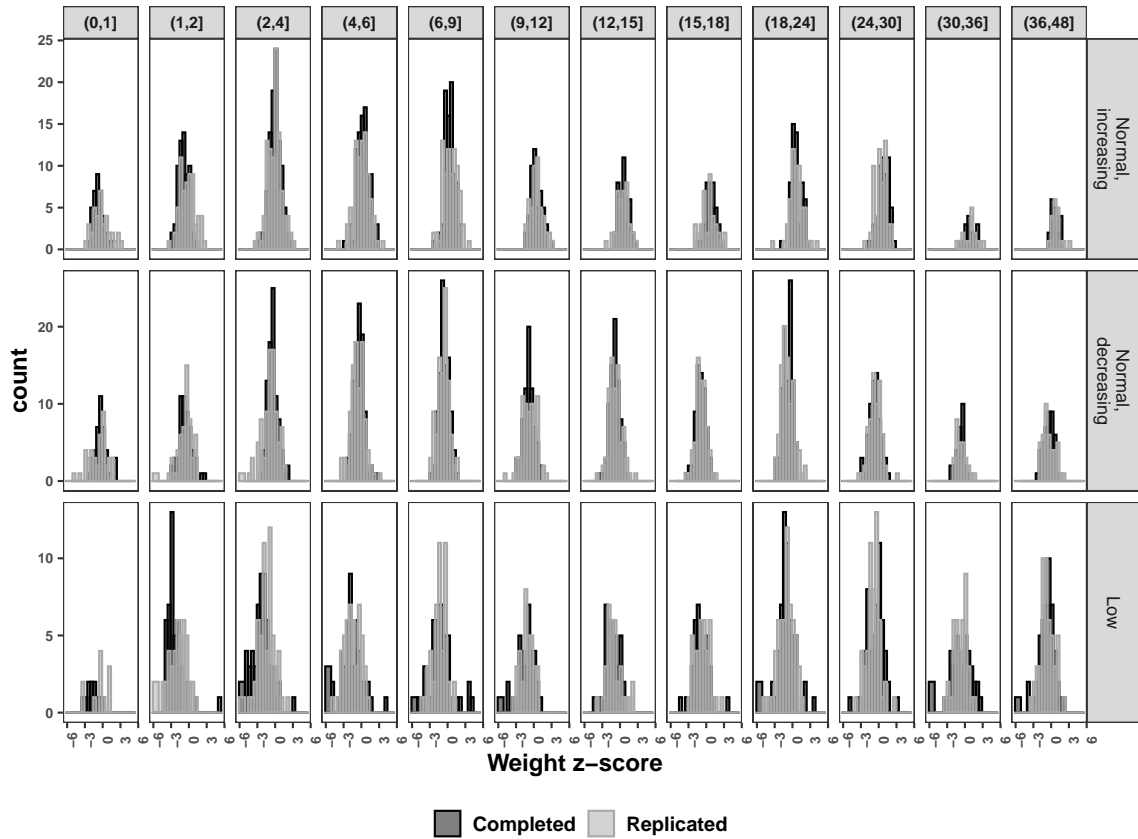


Figure B.6: Histograms of completed and replicated completed weight z-scores from the posterior predictive distribution, by subgroup and well-child window, assuming 3 latent classes and using the MNAR method.

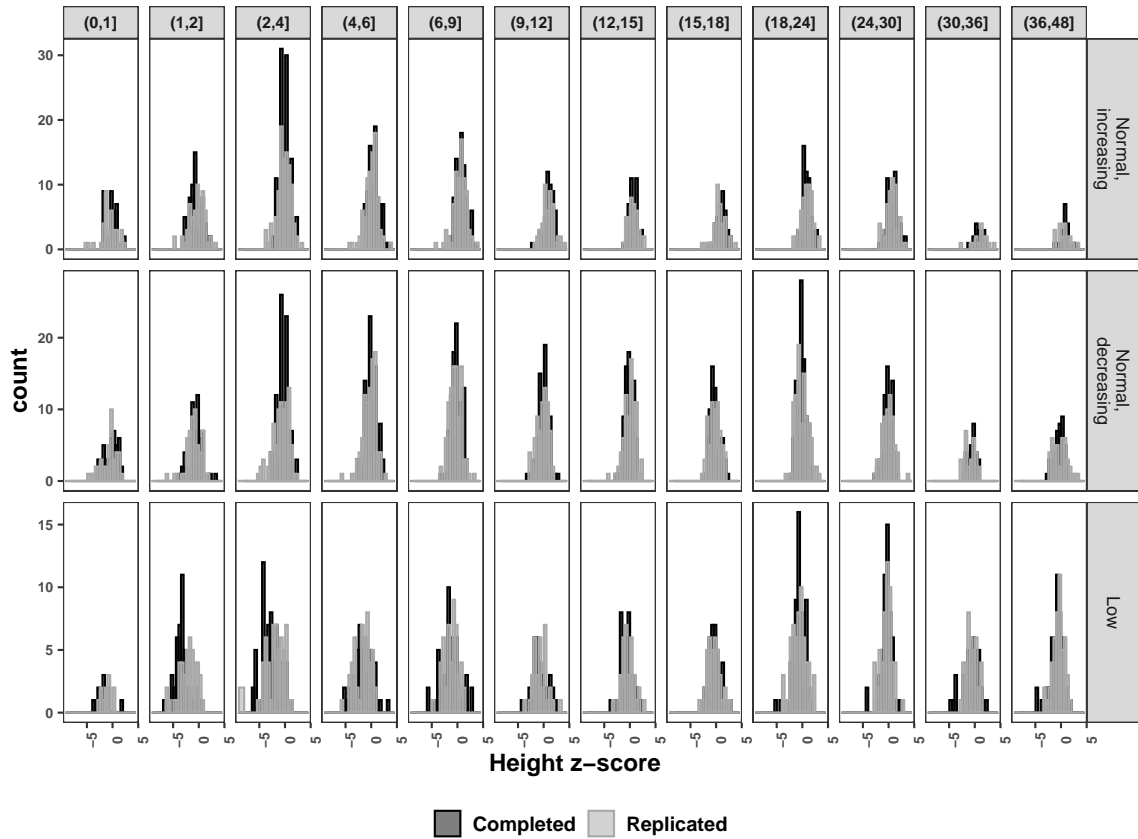


Figure B.7: Histograms of completed and replicated completed height z-scores from the posterior predictive distribution, by subgroup and well-child window, assuming 3 latent classes and using the MNAR method.

B.2 Child classification using the different estimation methods in 2-class models

The **Naïve**, **MAR**, and **MNAR** methods each detected a Normal trajectory subgroup (purple) and a Low trajectory subgroup (orange) (Figures B.8 and B.9).

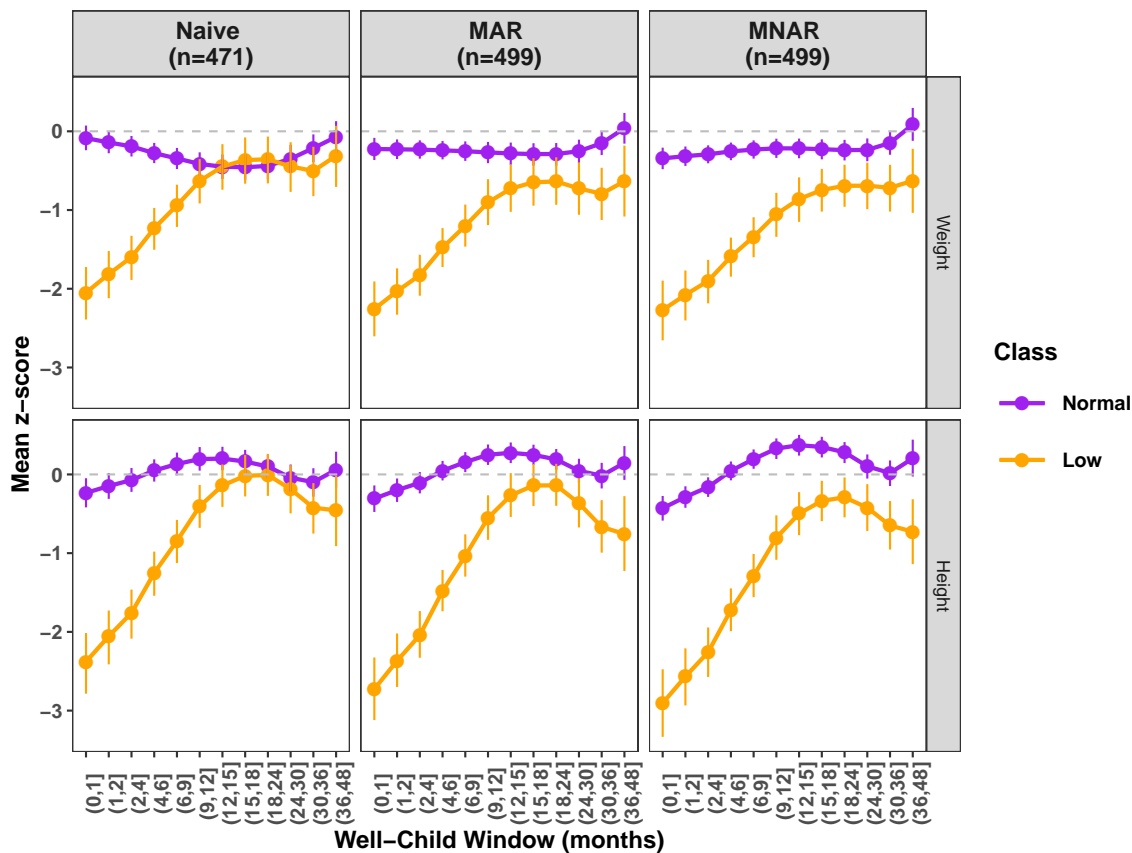


Figure B.8: Latent class-specific average trajectories of weight and height z-scores estimated by the **Naïve**, **MAR**, and **MNAR** methods, assuming 2 latent classes. n refers to the number of children included by each method.

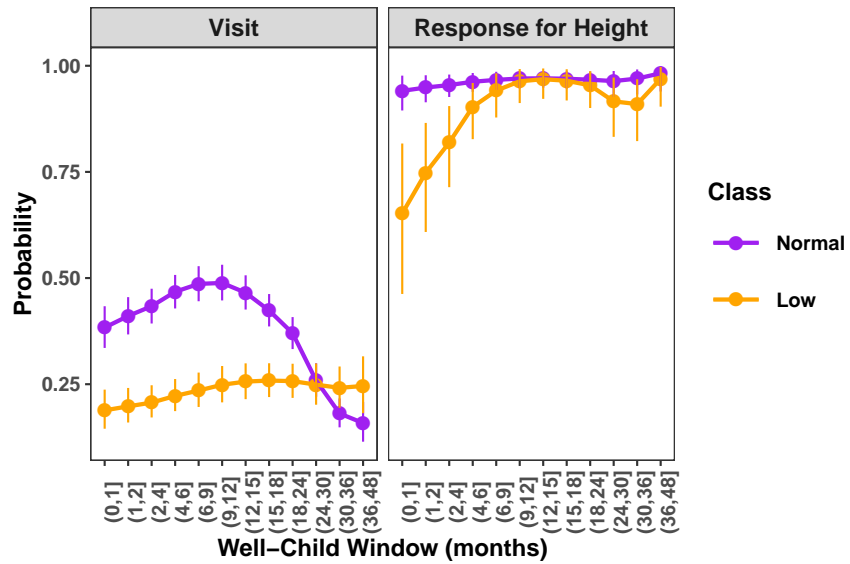


Figure B.9: Latent class-specific trajectories of the probability of a clinic visit and the probability of a response for height z-scores using the **MNAR** method, assuming 2 latent classes.

Table B.3 presents a summary of posterior latent class assignment under the three estimation methods. The **MNAR** method assigned about 8% fewer children to the Normal subgroup than the other methods. The mean (median) probability of latent class assignment in each subgroup ranged from 0.87 to 0.93 (0.92 to 0.99).

Table B.3: Posterior latent class assignment in the 2-class models based on assigning children to the Normal or Low trajectory subgroup according to the maximum of the mean posterior probabilities of class assignment. The **Naïve**, **MAR**, and **MNAR** methods are shown.

	Normal	Low
Naïve ($n = 471$):		
Predicted class size (%)	304 (65)	167 (35)
Mean probability	0.87	0.88
Median probability	0.92	0.97
MAR ($n = 499$):		
Predicted class size (%)	335 (67)	164 (33)
Mean probability	0.90	0.91
Median probability	0.96	0.99
MNAR ($n = 499$):		
Predicted class size (%)	292 (59)	207 (41)
Mean probability	0.93	0.87
Median probability	0.99	0.95

Table B.4 cross-classifies the 499 children by their latent class assignment from the **MAR** and **MNAR** methods, and the birth weight variable from the latent class membership model.

Table B.4: Cross-classification of 499 children assigned to the Normal and Low trajectory subgroups by the **MAR** and **MNAR** methods, according to low birth weight (LBW) status.

	MNAR			
	Non-LBW		LBW	
	Normal	Low	Normal	Low
MAR				
Normal	256	52	16	11
Low	17	58	3	86

C Simulation Study Addendum

C.1 Design

We designed the study based on the real data analysis with 2 latent classes estimated with the **MNAR** method. For $i = 1, \dots, 500$ subjects over $j = 1, \dots, 12$ time windows, we generated longitudinal outcomes of interest y_{1ij} and y_{2ij} , with about 60% and 40% of subjects in latent classes 1 and 2, respectively. We assumed the missing data mechanisms for the visit process and response process for y_2 are MNAR, while y_1 is fully observed given a clinic visit. In this setting, we considered the following five specific scenarios (S0-S4):

1. Under S0, we mimicked the latent class-specific trajectories and missingness proportions in the real data analysis. True parameter values for variance components were selected according to the real data analysis.

First, we generated the latent class membership of subject i as

$$\left[c_i \mid w_i \right] \sim \text{Bernoulli} \left(\pi_{i2} \right),$$

where using a probit link function, $\pi_{i2} = \Phi\{-0.25 - w_i\}$. π_{i2} is the probability that subject i belongs to latent class 2, and w_i is a scaled and centered simulated variable for a subject's birth weight.

Then, we generated the longitudinal outcomes, visit process, and response process given a

clinic visit conditional on a subject's latent class membership as

$$\begin{bmatrix} y_{1ij} \\ y_{2ij} \end{bmatrix} \Big| c_i = k \sim MVN_2 \left(\begin{bmatrix} \beta_{1k1} + \beta_{1k2}x_{ij} + b_{1i1} \\ \beta_{2k1} + \beta_{2k2}x_{ij} + b_{2i1} \end{bmatrix}, \boldsymbol{\Sigma}_k \right) \quad (5)$$

$$\begin{bmatrix} b_{1i1} \\ b_{2i1} \end{bmatrix} \Big| c_i = k \sim MVN_2 \left(\begin{bmatrix} 0 \\ 0 \end{bmatrix}, \begin{bmatrix} \Psi_{k1} & 0 \\ 0 & \Psi_{k2} \end{bmatrix} \right) \quad (6)$$

$$d_{ij} \Big| c_i = k \sim \text{Bernoulli} \left(\Phi\{\phi_{k1} + \phi_{k2}x_{ij} + \tau_{i1}\} \right) \quad (7)$$

$$\tau_{i1} \Big| c_i = k \sim \text{Normal} \left(0, 0.25 \right)$$

$$m_{2i,A(l)} \Big| c_i = k \sim \text{Bernoulli} \left(\Phi\{\lambda_{2k1} + \lambda_{2k2}x_{iA(l)} + \kappa_{2i1}\} \right) \quad (8)$$

$$\kappa_{2i1} \Big| c_i = k \sim \text{Normal} \left(0, \Theta_{2k} \right) \quad (9)$$

In (5), for y_{1ij} , in latent class 1, $\beta_{11} = (\beta_{111}, \beta_{112})^T = (-0.25, 0.1)$, and in latent class 2, $\beta_{12} = (\beta_{121}, \beta_{122})^T = (-1, 0.5)$. For y_{2ij} , $\beta_{21} = (\beta_{211}, \beta_{212})^T = (0.5, 0.2)$, and $\beta_{22} = (\beta_{221}, \beta_{222})^T = (-0.5, 0.75)$. The latent class-specific variance-covariances of y_{1ij} , y_{2ij} are $\boldsymbol{\Sigma}_1 = \begin{bmatrix} 0.5 & 0.2 \\ 0.2 & 0.5 \end{bmatrix}$ and $\boldsymbol{\Sigma}_2 = \begin{bmatrix} 1.5 & 1 \\ 1 & 1.5 \end{bmatrix}$. In (6), for the random intercept of y_{1ij} , the latent class-specific variances are $\Psi_{11} = \Psi_{21} = 0.6$. For y_{2ij} , $\Psi_{12} = 0.6$ and $\Psi_{22} = 0.4$.

For the visit process, in (7), $\phi_k = (\phi_{k1}, \phi_{k2})^T$, with $\phi_1 = (-0.2, -0.8)$ and $\phi_2 = (-0.8, 0.2)$.

For the response process of y_{2ij} given a clinic visit, in (8), $\lambda_{2k} = (\lambda_{2k1}, \lambda_{2k2})^T$, with $\lambda_{21} = (1.9, 0.1)$ and $\lambda_{22} = (1.1, 0.25)$. The latent class-specific random intercept variances (9) are $\Theta_{21} = 0.5$ and $\Theta_{22} = 1.5$.

Depicting y_1 and y_2 in S0, Figure C.1 shows that in early follow-up when the latent class-specific average trajectories are better separated, missingness in y_2 is high in class 2, while in later follow-up, missingness in y_2 is high in class 1.

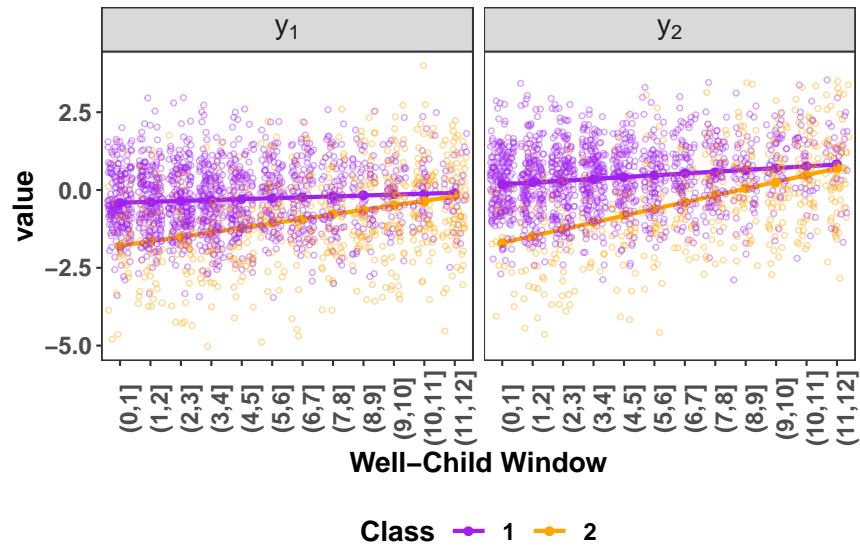


Figure C.1: Average latent class-specific trajectories for y_1 and y_2 overlaid by points for observed measurements, under S_0 .

2. In S1, we modified S0 by increasing the difference in the slopes for the latent class-specific trajectories of y_2 : We made the slope in latent class 2 steeper. Specifically, in (5), $\beta_{222} = 1$. No other changes to S0 were made.
3. In S2, we modified S0 by decreasing the difference in the slopes for the latent class-specific trajectories of y_2 : We made the slope in latent class 2 nearly parallel to the latent class 1 slope. Specifically, in (5), $\beta_{222} = 0.3$. No other changes to S0 were made.
4. In S3, we altered the visit process of S0 to reduce the percent of missed clinic visits in each latent class whilst maintaining the general visit process trajectory. In (7), we set $\phi_1 = (0.4, -0.2)$ and $\phi_2 = (-0.1, 0.9)$. These changes resulted in 35% missed clinic visits in latent class 1, and 55% missed clinic visits in latent class 2. No other changes to S0 were made.
5. In S4, we modified S0 by increasing the percent of missed responses of y_2 in each latent class whilst maintaining the general response process trajectory. In (8), we set $\lambda_{21} = (0.8, 0.1)$ and $\lambda_{22} = (0.5, 0.2)$. These changes resulted in 25% missed responses in y_2 in latent class 1, and 35% missed responses in y_2 in latent class 2. No other changes to S0 were made.

Figure C.2 portrays S1 – S4 for y_2 .

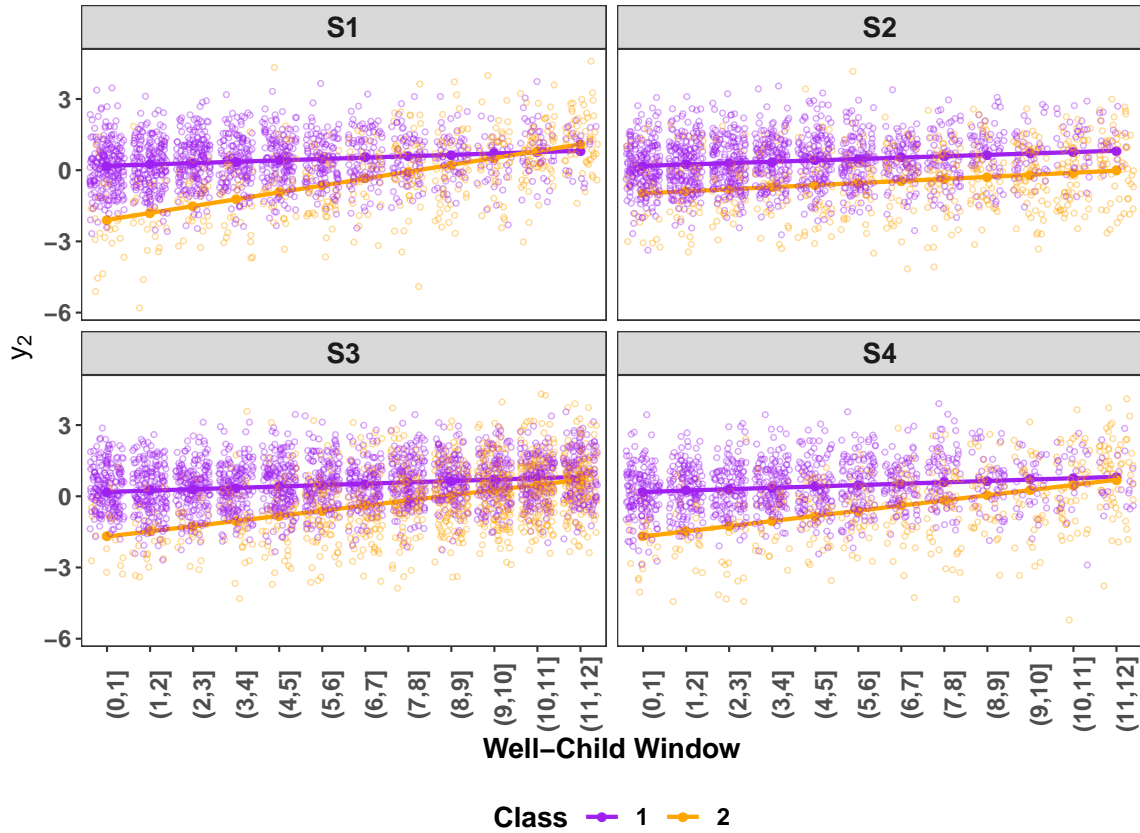


Figure C.2: Average latent class-specific trajectories for y_2 overlaid by points for observed measurements, under S1 to S4. Compared to S0, in S1, the latent class-specific slopes are more different. In S2, they are more similar. In S3, the percent of missed clinic visits is reduced compared to S0. In S4, the percent of missed responses given a clinic visit is increased compared to S0.

C.2 Results

Table C.1: Simulation results of S1 for parameter estimation of intercept β_{rk1} and slope β_{rk2} for longitudinal outcome r in latent class k , along with the corresponding marginal intercept and slope, $\tilde{\beta}_{r1}$ and $\tilde{\beta}_{r2}$, respectively, under the **Full**, **Naïve**, **MAR**, and **MNAR** methods. The **Full** method is the benchmark. The best performing method among the **Naïve**, **MAR**, and **MNAR** methods is in bold.

Outcome	Parameter	Method	Truth	Bias	MSE	Coverage	Length	
y_1	β_{111} (Class 1 Intercept)	Full		0.002	0.002	0.960	0.188	
		Naïve	-0.250	0.018	0.004	0.930	0.217	
		MAR		0.006	0.003	0.948	0.212	
		MNAR		0.005	0.003	0.946	0.209	
	β_{121} (Class 2 Intercept)	Full		-1.000	-0.003	0.003	0.952	0.228
		Naïve			0.005	0.014	0.922	0.404
		MAR			-0.010	0.009	0.946	0.369
	β_{112} (Class 1 Slope)	MNAR			0.006	0.007	0.932	0.314
		Full		0.100	-0.000	0.000	0.940	0.048
		Naïve			-0.008	0.001	0.936	0.096
	β_{122} (Class 2 Slope)	MAR			-0.006	0.001	0.950	0.092
		MNAR			0.000	0.001	0.946	0.091
Full			0.500	-0.001	0.001	0.946	0.096	
y_2	β_{211} (Class 1 Intercept)	Naïve		0.029	0.004	0.894	0.214	
		MAR	0.500	0.029	0.004	0.914	0.212	
		MNAR		0.009	0.003	0.932	0.209	
		Full			-0.004	0.003	0.942	0.194
	β_{221} (Class 2 Intercept)	Naïve		-0.500	0.039	0.014	0.890	0.380
		MAR			0.025	0.011	0.916	0.364
		MNAR			0.009	0.008	0.934	0.311
	β_{212} (Class 1 Slope)	Full		0.200	0.001	0.000	0.946	0.048
		Naïve			-0.013	0.001	0.904	0.095
		MAR			-0.011	0.001	0.902	0.094
	β_{222} (Class 2 Slope)	MNAR			0.002	0.001	0.934	0.093
		Full		1.000	0.001	0.001	0.944	0.097
Naïve				-0.062	0.012	0.814	0.287	
y_1	$\tilde{\beta}_{11}$ (Marginal Intercept)	MAR		-0.034	0.007	0.896	0.275	
		MNAR		-0.008	0.004	0.954	0.239	
		Full		-0.582	-0.001	0.001	0.950	0.147
		Naïve			0.070	0.008	0.653	0.183
	$\tilde{\beta}_{12}$ (Marginal Slope)	MAR			0.049	0.004	0.807	0.176
		MNAR			0.019	0.003	0.915	0.177
		Full		0.277	-0.000	0.000	0.962	0.051
	$\tilde{\beta}_{21}$ (Marginal Intercept)	Naïve			-0.056	0.004	0.501	0.110
		MAR			-0.037	0.002	0.695	0.101
		MNAR			-0.009	0.001	0.909	0.104
	$\tilde{\beta}_{22}$ (Marginal Slope)	Full		0.058	-0.002	0.001	0.948	0.138
		Naïve			0.108	0.014	0.359	0.178
MAR				0.094	0.011	0.450	0.177	
$\tilde{\beta}_{22}$ (Marginal Slope)	MNAR			0.028	0.003	0.857	0.177	
	Full		0.554	0.001	0.000	0.932	0.056	
	Naïve			-0.092	0.010	0.144	0.113	
$\tilde{\beta}_{22}$ (Marginal Slope)	MAR			-0.073	0.006	0.279	0.112	
	MNAR			-0.018	0.001	0.865	0.115	

Table C.2: Simulation results of S2 for parameter estimation of intercept β_{rk1} and slope β_{rk2} for longitudinal outcome r in latent class k , along with the corresponding marginal intercept and slope, $\tilde{\beta}_{r1}$ and $\tilde{\beta}_{r2}$, respectively, under the **Full**, **Naïve**, **MAR**, and **MNAR** methods. The **Full** method is the benchmark. The best performing method among the **Naïve**, **MAR**, and **MNAR** methods is in bold.

Outcome	Parameter	Method	Truth	Bias	MSE	Coverage	Length		
y_1	β_{111} (Class 1 Intercept)	Full		0.003	0.002	0.942	0.190		
		Naïve	-0.250	0.054	0.007	0.832	0.231		
		MAR		0.036	0.005	0.890	0.225		
		MNAR		0.001	0.003	0.956	0.209		
	β_{121} (Class 2 Intercept)	Full		-1.000	-0.003	0.003	0.950	0.231	
		Naïve			0.057	0.016	0.885	0.397	
		MAR			0.025	0.010	0.928	0.366	
	β_{112} (Class 1 Slope)	MNAR			0.008	0.006	0.962	0.314	
		Full		0.100	-0.000	0.000	0.948	0.048	
		Naïve			-0.014	0.001	0.913	0.101	
	β_{122} (Class 2 Slope)	MAR			-0.012	0.001	0.934	0.096	
		MNAR			-0.002	0.001	0.960	0.091	
Full			0.500	0.000	0.001	0.938	0.097		
y_2	β_{211} (Class 1 Intercept)	Naïve		0.038	0.006	0.866	0.236		
		MAR	0.500	0.034	0.005	0.866	0.231		
		MNAR		0.009	0.003	0.936	0.210		
		Full			-0.003	0.002	0.950	0.197	
	β_{221} (Class 2 Intercept)	Naïve		-0.500	0.023	0.010	0.929	0.363	
		MAR			0.008	0.009	0.932	0.349	
		MNAR			0.014	0.007	0.932	0.310	
	β_{212} (Class 1 Slope)	Full		0.200	-0.000	0.000	0.940	0.048	
		Naïve			-0.008	0.001	0.917	0.099	
		MAR			-0.008	0.001	0.942	0.098	
	β_{222} (Class 2 Slope)	MNAR			0.001	0.001	0.932	0.093	
		Full		0.300	-0.001	0.001	0.942	0.096	
Naïve				-0.102	0.014	0.597	0.236		
y_1	$\tilde{\beta}_{11}$ (Marginal Intercept)	MAR		-0.077	0.010	0.726	0.233		
		MNAR		-0.000	0.003	0.944	0.235		
		Full			-0.000	0.001	0.952	0.147	
	$\tilde{\beta}_{12}$ (Marginal Slope)	Naïve		-0.582	0.086	0.010	0.524	0.182	
		MAR			0.058	0.006	0.742	0.175	
		MNAR			0.017	0.002	0.946	0.176	
	y_2	$\tilde{\beta}_{21}$ (Marginal Intercept)	Full		0.000	0.000	0.956	0.051	
			Naïve		0.277	-0.068	0.006	0.318	0.108
			MAR			-0.047	0.003	0.542	0.100
		$\tilde{\beta}_{22}$ (Marginal Slope)	MNAR			-0.009	0.001	0.934	0.104
			Full		0.057	-0.001	0.001	0.946	0.139
			Naïve			0.073	0.008	0.595	0.173
$\tilde{\beta}_{22}$ (Marginal Slope)	MAR			0.058	0.006	0.718	0.173		
	MNAR			0.028	0.003	0.888	0.176		
	Full		0.244	-0.001	0.000	0.930	0.050		
$\tilde{\beta}_{22}$ (Marginal Slope)	Naïve			-0.050	0.003	0.518	0.104		
	MAR			-0.040	0.002	0.670	0.104		
	MNAR			-0.001	0.001	0.948	0.111		

Table C.3: Simulation results of S3 for parameter estimation of intercept β_{rk1} and slope β_{rk2} for longitudinal outcome r in latent class k , along with the corresponding marginal intercept and slope, $\tilde{\beta}_{r1}$ and $\tilde{\beta}_{r2}$, respectively, under the **Full**, **Naïve**, **MAR**, and **MNAR** methods. The **Full** method is the benchmark. The best performing method among the **Naïve**, **MAR**, and **MNAR** methods is in bold.

Outcome	Parameter	Method	Truth	Bias	MSE	Coverage	Length		
y_1	β_{111} (Class 1 Intercept)	Full		-0.002	0.002	0.950	0.190		
		Naïve	-0.250	0.008	0.003	0.954	0.199		
		MAR		-0.001	0.003	0.946	0.197		
		MNAR		-0.001	0.002	0.958	0.195		
	β_{121} (Class 2 Intercept)	Full			0.000	0.003	0.956	0.230	
		Naïve	-1.000		0.014	0.009	0.922	0.338	
		MAR			0.001	0.007	0.944	0.307	
	β_{112} (Class 1 Slope)	MNAR			0.008	0.005	0.940	0.274	
		Full			-0.000	0.000	0.930	0.048	
		Naïve	0.100		-0.004	0.000	0.944	0.066	
	β_{122} (Class 2 Slope)	MAR			-0.004	0.000	0.930	0.064	
		MNAR			0.001	0.000	0.938	0.062	
Full				0.001	0.001	0.930	0.096		
y_2	β_{211} (Class 1 Intercept)	Naïve	0.500		-0.040	0.005	0.878	0.222	
		MAR			-0.017	0.003	0.924	0.194	
		MNAR			-0.004	0.002	0.968	0.176	
		Full			-0.000	0.002	0.954	0.189	
	β_{221} (Class 2 Intercept)	Naïve	-0.500		0.008	0.003	0.946	0.199	
		MAR			0.006	0.003	0.936	0.198	
		MNAR			0.003	0.003	0.952	0.195	
	β_{212} (Class 1 Slope)	Full			-0.003	0.003	0.940	0.196	
		Naïve	-0.500		0.011	0.007	0.938	0.311	
		MAR			0.010	0.007	0.918	0.296	
	β_{222} (Class 2 Slope)	MNAR			0.010	0.005	0.924	0.263	
		Full			-0.001	0.000	0.918	0.048	
Naïve		0.200		-0.007	0.000	0.916	0.066		
y_1	$\tilde{\beta}_{11}$ (Marginal Intercept)	MAR		-0.008	0.000	0.918	0.065		
		MNAR			0.000	0.000	0.944	0.064	
		Full			0.001	0.001	0.934	0.097	
	$\tilde{\beta}_{12}$ (Marginal Slope)	Naïve	0.750		-0.044	0.006	0.872	0.223	
		MAR			-0.031	0.004	0.885	0.212	
		MNAR			-0.007	0.003	0.928	0.190	
	y_2	$\tilde{\beta}_{21}$ (Marginal Intercept)	Full		-0.001	0.001	0.950	0.147	
			Naïve	-0.582		0.043	0.004	0.794	0.168
			MAR			0.025	0.003	0.887	0.161
			MNAR			0.001	0.002	0.934	0.162
		$\tilde{\beta}_{22}$ (Marginal Slope)	Full			0.000	0.000	0.952	0.051
			Naïve	0.277		-0.036	0.002	0.646	0.092
MAR					-0.023	0.001	0.805	0.084	
$\tilde{\beta}_{21}$ (Marginal Intercept)		MNAR			0.000	0.000	0.954	0.086	
		Full			-0.001	0.001	0.954	0.138	
		Naïve	0.057		0.053	0.005	0.742	0.161	
$\tilde{\beta}_{22}$ (Marginal Slope)		MAR			0.041	0.004	0.785	0.160	
		MNAR			0.003	0.002	0.909	0.160	
	Full			-0.000	0.000	0.944	0.053		
$\tilde{\beta}_{22}$ (Marginal Slope)	Naïve	0.444		-0.046	0.003	0.476	0.092		
	MAR			-0.036	0.002	0.652	0.091		
	MNAR			-0.001	0.001	0.909	0.092		

Table C.4: Simulation results of S4 for parameter estimation of intercept β_{rk1} and slope β_{rk2} for longitudinal outcome r in latent class k , along with the corresponding marginal intercept and slope, $\tilde{\beta}_{r1}$ and $\tilde{\beta}_{r2}$, respectively, under the **Full**, **Naïve**, **MAR**, and **MNAR** methods. The **Full** method is the benchmark. The best performing method among the **Naïve**, **MAR**, and **MNAR** methods is in bold.

Outcome	Parameter	Method	Truth	Bias	MSE	Coverage	Length	
y_1	β_{111} (Class 1 Intercept)	Full		-0.002	0.002	0.950	0.190	
		Naïve	-0.250	0.046	0.007	0.870	0.249	
		MAR		0.034	0.004	0.900	0.222	
		MNAR		0.005	0.003	0.964	0.210	
	β_{121} (Class 2 Intercept)	Full		-1.000	0.000	0.003	0.956	0.230
		Naïve			0.091	0.024	0.830	0.424
		MAR			0.015	0.011	0.928	0.374
		MNAR			0.010	0.006	0.942	0.316
	β_{112} (Class 1 Slope)	Full		0.100	-0.000	0.000	0.930	0.048
		Naïve			-0.012	0.001	0.920	0.117
		MAR			-0.009	0.001	0.930	0.095
		MNAR			-0.002	0.001	0.950	0.091
β_{122} (Class 2 Slope)	Full		0.500	0.001	0.001	0.930	0.096	
	Naïve			-0.122	0.022	0.590	0.282	
	MAR			-0.052	0.007	0.846	0.235	
	MNAR			-0.003	0.003	0.952	0.216	
y_2	β_{211} (Class 1 Intercept)	Full		-0.000	0.002	0.954	0.189	
		Naïve	0.500	0.076	0.011	0.754	0.250	
		MAR		0.045	0.006	0.888	0.233	
		MNAR		0.009	0.004	0.922	0.220	
	β_{221} (Class 2 Intercept)	Full		-0.500	-0.003	0.003	0.940	0.196
		Naïve			0.096	0.025	0.778	0.405
		MAR			0.049	0.015	0.874	0.388
		MNAR			0.003	0.007	0.950	0.334
	β_{212} (Class 1 Slope)	Full		0.200	-0.001	0.000	0.918	0.048
		Naïve			-0.020	0.001	0.882	0.116
		MAR			-0.016	0.001	0.898	0.109
		MNAR			-0.003	0.001	0.930	0.105
β_{222} (Class 2 Slope)	Full		0.750	0.001	0.001	0.934	0.097	
	Naïve			-0.148	0.030	0.478	0.285	
	MAR			-0.084	0.014	0.740	0.280	
	MNAR			-0.004	0.004	0.976	0.258	
y_1	$\tilde{\beta}_{11}$ (Marginal Intercept)	Full		-0.001	0.001	0.950	0.147	
		Naïve	-0.582	0.097	0.012	0.512	0.191	
		MAR		0.063	0.006	0.696	0.175	
		MNAR		0.020	0.003	0.903	0.177	
	$\tilde{\beta}_{12}$ (Marginal Slope)	Full		0.277	0.000	0.000	0.952	0.051
		Naïve			-0.074	0.007	0.360	0.120
		MAR			-0.046	0.003	0.574	0.100
		MNAR			-0.009	0.001	0.918	0.105
	$\tilde{\beta}_{21}$ (Marginal Intercept)	Full		0.057	-0.001	0.001	0.954	0.138
		Naïve			0.127	0.019	0.236	0.185
		MAR			0.094	0.012	0.494	0.184
		MNAR			0.023	0.003	0.901	0.187
$\tilde{\beta}_{22}$ (Marginal Slope)	Full		0.444	-0.000	0.000	0.944	0.053	
	Naïve			-0.096	0.010	0.174	0.120	
	MAR			-0.070	0.006	0.374	0.118	
	MNAR			-0.013	0.001	0.940	0.124	

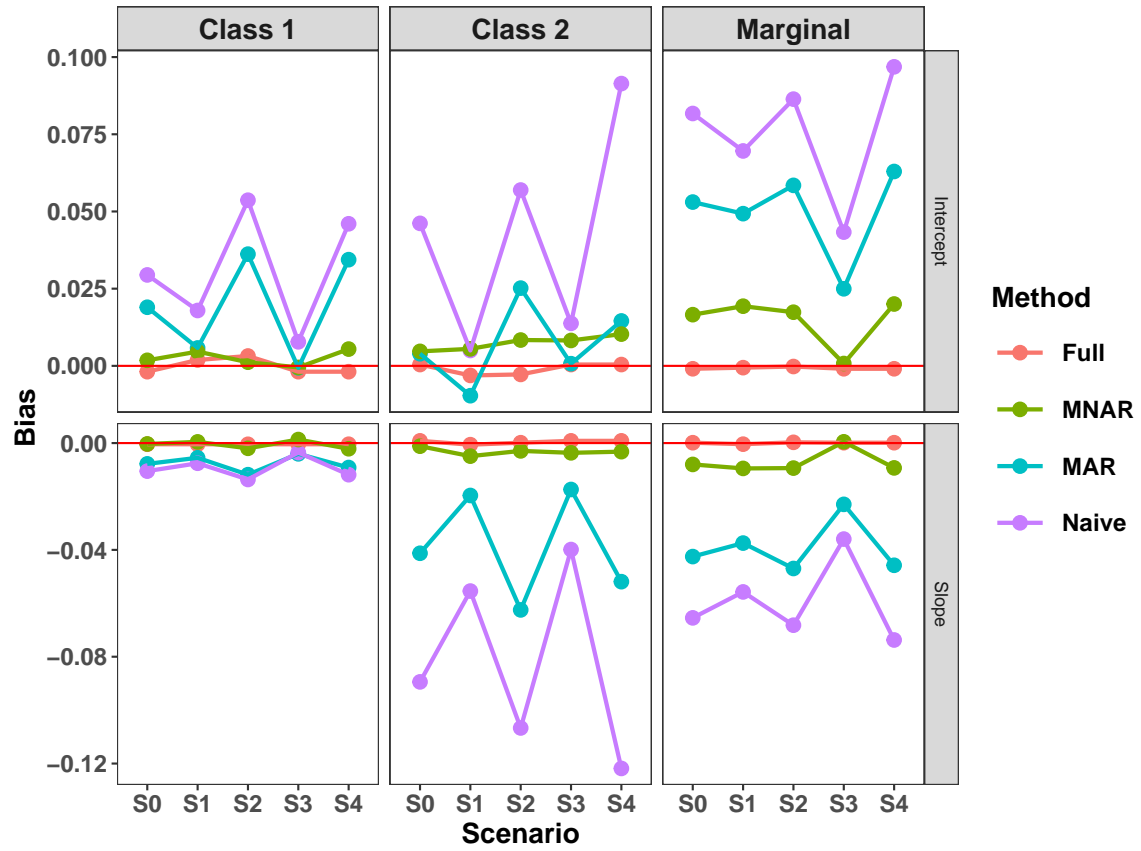


Figure C.3: Comparison of bias in parameter estimation for y_1 across data generation scenarios, by estimation method.

Table C.5: Simulation results for subject misclassification by data generation scenario under the **Full**, **Naïve**, **MAR**, and **MNAR** methods. The **Full** method is the benchmark. The best performing method among the **Naïve**, **MAR**, and **MNAR** methods is in bold.

Scenario	Method	Min	Percentile			Max
			25	50	75	
S0	Full	0.00	0.01	0.02	0.02	0.04
	Naïve	0.09	0.14	0.15	0.16	0.20
	MAR	0.09	0.13	0.14	0.16	0.20
	MNAR	0.01	0.03	0.03	0.04	0.06
S1	Full	0.00	0.01	0.01	0.01	0.03
	Naïve	0.09	0.12	0.13	0.14	0.19
	MAR	0.08	0.12	0.13	0.14	0.18
	MNAR	0.01	0.02	0.03	0.03	0.06
S2	Full	0.00	0.02	0.02	0.03	0.05
	Naïve	0.08	0.14	0.15	0.17	0.22
	MAR	0.10	0.13	0.14	0.16	0.20
	MNAR	0.01	0.03	0.03	0.04	0.06
S3	Full	0.00	0.01	0.02	0.02	0.04
	Naïve	0.07	0.10	0.11	0.12	0.16
	MAR	0.06	0.09	0.10	0.11	0.14
	MNAR	0.00	0.02	0.02	0.02	0.04
S4	Full	0.00	0.01	0.02	0.02	0.04
	Naïve	0.11	0.15	0.17	0.18	0.25
	MAR	0.11	0.14	0.15	0.17	0.21
	MNAR	0.01	0.03	0.04	0.04	0.07

D R package EHRMiss

Our R package EHRMiss is available for download at <https://github.com/anthopolos/EHRMiss>.

We provide an example of how to use the package to implement the proposed model for longitudinal health outcomes in EHRs with a nonignorable visit process and response process given a clinic visit.

```
#----- Load data from the EHRMiss package
data(data)
names(data)
dim(data)

#----- Model details
### Number of outcomes
J <- 2
### Number of latent classes
K <- 2

#----- Specify the formulas for the design matrices and put the formulas in
↔ regf
regf <- list(LatentClass = ~ 1 + birthweight,
             YRe = ~ 1,
             YObs = ~ -1 + time,
             YSub = ~ 1,
             DObs = ~ 1 + time,
             DRe = ~ 1,
             MObs = ~ 1 + time,
             MRe = ~ 1)
```

```

#----- MCMC preparation
m <- length(all.vars(regf[["LatentClass"]])) + 1
p <- length(all.vars(regf[["YSub"]])) + 1
s <- length(all.vars(regf[["YObs"]]))
f <- length(all.vars(regf[["DObs"]])) + 1
e <- length(all.vars(regf[["MObs"]])) + 1

### Number of random effects, assumed the same for all models
q <- length(all.vars(regf[["YRe"]])) + 1

### Prior distributions
priors <- list(list(rep(0, m), diag(1, m)), list(rep(0, s), diag(100, s)),
              list(rep(0, p), diag(10000, p)),
              list(1, 1),
              list(diag(c(0.5, 0.6), J), (J + 2)),
              list(rep(0, f), diag(100, f)),
              list(1, 1),
              list(rep(0, e), diag(100, e)),
              list(scale = 1, df = 1))

### Initial values
inits <- list(matrix(rep(0, m * (K - 1)), nrow = m, ncol = (K - 1)),
              list(matrix(rnorm(s*K), ncol = K, nrow = s), matrix(rnorm(s*K), ncol
                ↪ = K, nrow = s)),
              list(array(rnorm(p*q*K), dim = c(p, q, K)), array(rnorm(p*q*K), dim =
                ↪ c(p, q, K))),
              list(array(rep(0.4, K), dim = c(q, q, K)), array(rep(0.4, K), dim =
                ↪ (q, q, K))),
              array(c(1, 0, 0, 1, 0.5, 0, 0, 0.5), dim = c(J, J, K)),

```

```

matrix(rnorm(f*K), ncol = K),
array(rep(0.5, K), dim = c(q, q, K)),
list(matrix(rnorm(e*K), ncol = K)),
list(array(rep(0.5, K), dim = c(q, q, K))))

#----- Fit model with MNAR visit process, MNAR response process for Y2, Y1
  ↪ fully observed given a clinic visit
n.samples <- 2000
burn <- 1000
update <- 10
monitor <- TRUE

#MNAR Visit process
#MNAR response process for Y2
#See ?MVNYBinaryMiss
res <- MVNYBinaryMiss(K = K, J = J, data = data, regf = regf, imputeResponse =
  ↪ TRUE, Mvec = 2, modelVisit = TRUE, modelResponse = TRUE, priors = priors,
  ↪ inits = inits, n.samples = n.samples, burn = burn, monitor = monitor,
  ↪ update = update, modelComparison = TRUE, sims = FALSE)

#Printed to console: posterior summaries of model parameters, posterior latent
  ↪ class membership, model comparison statistics, label switching diagnostic

#Get Bayesian posterior predictive p-value, see ?get_discrepancy_plot
#Set working directory to where discrepancy samples are written
store_T_completed <- read.table("store_T_completed.txt", header = FALSE, sep = ",
  ↪ ")

```

```
get_discrepancy_plot(store_T_completed)
```

References

- J. Albert and S. Chib. Bayesian Analysis of Binary and Polychotomous Response Data. *Journal of the American Statistical Association*, 88(422):669–679, 1993.
- G. Celeux, F. Forbes, C. P. Robert, and D. M. Titterton. Deviance Information Criteria for Missing Data Models. *Bayesian Analysis*, 1(4):651–674, 2006.
- E. S. Garrett and S. L. Zeger. Latent Class Model Diagnosis. *Biometrics*, 56:1055–1067, 2000.
- S. Geisser and W. F. Eddy. A Predictive Approach to Model Selection. *Journal of the American Statistical Association*, 74:153–160, 1979.
- A. E. Gelfand and D. K. Dey. Bayesian Model Choice: Asymptotics and Exact Calculations. *Journal of the Royal Statistical Society. Series B (Methodological)*, 56(3):501–514, 1994.
- A. E. Gelfand, S. K. Sahu, and B. P. Carlin. Efficient Parametrisations for Normal Linear Mixed Models. *Biometrika*, 82(3):479–488, 1995.
- A. E. Gelfand, S. K. Sahu, and B. P. Carlin. Efficient Parametrizations for Generalized Linear Mixed Models, (with discussion). In J. M. Bernardo, J. O. Berger, and A. P. Dawid, editors, *Bayesian Statistics 5*, pages 165–180. Clarendon Press, 1996. URL <http://www.maths.soton.ac.uk/staff/Sahu/papers/gsc2.html>.
- A. Gelman, J. B. Carlin, H. S. Stern, and D. B. Rubin. *Bayesian Data Analysis*, volume 2. Taylor & Francis, 2014.
- J. G. Ibrahim, M. Chen, and D. Sinha. Model Comparison. In *Bayesian Survival Analysis*, pages 208–261. Springer Science Business Media, LLC, New York, 2001.
- R. H. Jones. Bayesian Information Criterion for Longitudinal and Clustered Data. *Statistics in Medicine*, 30:3050–3056, 2011.

- R. McCulloch and P. E. Rossi. An Exact Likelihood Analysis of the Multinomial Probit Model. *Journal of Econometrics*, 64:207–240, 1994.
- G. Schwarz. Estimating the Dimension of a Model. *The Annals of Statistics*, 6(2):461–464, 1978.
- D. J. Spiegelhalter, N. G. Best, B. P. Carlin, and A. Linde. Bayesian Measures of Model Complexity and Fit. *Journal of the Royal Statistical Society, B Methodology*, 64(4):583–639, 2002.
- M. A. Tanner and W. H. Wong. The Calculation of Posterior Distributions by Data Augmentation. *Journal of the American Statistical Association*, 82(398):528–540, 1987.